Euro. Jnl of Applied Mathematics (2004), *vol.* 15, *pp.* 451–486. © 2004 Cambridge University Press
DOI: 10.1017/S0956792504005595 Printed in the United Kingdom

One-dimensional magnetic domain walls

CARLOS J. GARCÍA-CERVERA

Department of Mathematics, University of California, Santa Barbara, CA 93106, USA
email: cgarcia@math.ucsb.edu

(*Received 30 May 2003; revised 14 November 2003*)

Ferromagnetic materials may present a complicated domain structure, due in part to the nonlocal nature of the self interactions. In this article we present a detailed study of the structure of one-dimensional magnetic domain walls in uniaxial ferromagnetic materials, and in particular, of the Néel and Bloch walls. We analyze the logarithmic tail of the Néel wall, and identify the characteristic length scales in both the Néel and Bloch walls. This analysis is used to obtain the optimal energy scaling for the Néel and Bloch walls. Our results are illustrated with numerical simulations of one-dimensional walls. A new model for the study of ferromagnetic thin films is presented.

1 Introduction

The micromagnetics model introduced by Landau & Lifshitz [20] for the study of ferromagnetic materials leads to a non-convex, non-local variational problem. The magnetic domain structure, characteristic of these materials, is understood in the context of energy minimization. The Landau-Lifshitz energy functional for a material occupying a volume V, in non-dimensional variables, is

$$F[\mathbf{m}] = \frac{q}{2}\int_V \Phi(\mathbf{m})\,dx + \frac{1}{2}\int_V |\nabla \mathbf{m}|^2\,dx - \frac{1}{2}\int_V \nabla u\cdot\mathbf{m}\,dx. \tag{1.1}$$

In (1.1), $|\mathbf{m}| = 1$ inside V, $\mathbf{m} = 0$ outside V, $|\nabla\mathbf{m}|^2$ is the exchange energy, q is the quality factor and $\Phi(\mathbf{m})$ is the energy due to material anisotropy. In this paper we consider uniaxial materials and we take the 'easy' axis as our OZ axis, i.e. $\Phi(\mathbf{m}) = m_1^2 + m_2^2$. The quality factor is defined as $q = K_u/(\mu_0 M_s^2)$, where K_u is the anisotropy constant, M_s is the saturation magnetization, and μ_0 is the permeability of vacuum. Finally, the last term in (1.1) is the energy due to the field induced by the magnetization distribution inside the material. This induced field $\mathbf{h}_s = -\nabla u$ can be computed by solving

$$\Delta u = \begin{cases} \nabla\cdot\mathbf{m} & \text{in } V,\\ 0 & \text{outside } V, \end{cases} \tag{1.2}$$

together with the jump conditions

$$[u] = 0, \tag{1.3}$$

$$\left[\frac{\partial u}{\partial v}\right] = -\mathbf{m}\cdot v, \tag{1.4}$$

Downloaded from https://www.cambridge.org/core. Lehrst F Alte Geschichte Hist Inst, on 06 Jun 2017 at 07:46:52, subject to the Cambridge Core terms of use, available at https://www.cambridge.org/core/terms. https://doi.org/10.1017/S0956792504005595

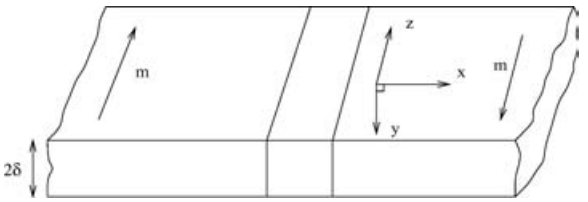

FIGURE 1. One-dimensional wall setting.

at the material-vacuum interface. In (1.3) and (1.4) we denote by [ ] the jump of a quantity across the interface. The vector ν represents the outward unit normal on the boundary of V. Lengths are measured in units of the characteristic length $l = \sqrt{A/(\mu_0 M_s^2)}$, where A is the material exchange constant, and energy is measured in units of $e = \sqrt{\mu_0 A M_s^2}$.

A brief explanation of the different terms involved in (1.1) is appropriate here. For a more detailed description, see Brown [3] and Hubert & Schäfer [19].

It has been observed experimentally that for sufficiently small samples of a ferromagnetic material, the intensity of magnetization per unit volume is constant. This constant is defined as the saturation magnetization, M_s. It has also been observed that crystalline materials are easier to magnetize in certain directions. For a uniaxial material there is one such direction of easy magnetization, or 'easy' axis. The anisotropy energy penalizes the deviations of $\mathbf{m}$ from this 'easy' direction. The quality factor is a measure of the relative strength of the anisotropy and the self-induced field energies. The exchange energy penalizes spatial deviations in $\mathbf{m}$, and it is responsible for the alignment of the spins that induces the ferromagnetic order in the material.

Functional (1.1) possesses a very rich energy landscape, and it has been the focus of recent attention in the mathematical community [9, 16, 18, 4, 5, 10, 11]. The local minimizers can present very complex structures [19, 10]. Rigorous bounds for functional (1.1) were presented in Choksi & Kohn [4] and Choksi *et al.* [5], and magnetic microstructures were analyzed in De Simone [9], Hubert [18] and De Simone *et al.* [10, 11]. In this work we analyze one-dimensional walls, which are part of the building blocks of more complicated structures. The results presented here have been recently used in the study of the cross-tie wall [11].

We assume that the magnetization depends only on the variable x, and that there is no structure in the direction *along* the wall (which is parallel to the easy axis). The OY direction represents the thickness of the film, as shown in Figure 1. Throughout this article we use the notation $\mathbf{e}_1 = (1,0,0)$, $\mathbf{e}_2 = (0,1,0)$, and $\mathbf{e}_3 = (0,0,1)$.

In this paper, we analyze the following model, introduced by Aharoni [1] for the study of one-dimensional magnetic domain walls:

$$F_{q,\delta}[\mathbf{m}] = \frac{q}{2}\int_{\mathbb{R}} \left(m_1^2 + m_2^2\right) + \frac{1}{2}\int_{\mathbb{R}} |\mathbf{m}'|^2 + \frac{1}{2}\int_{\mathbb{R}} \left(m_1^2 - m_1(\Gamma_\delta * m_1)\right) + \frac{1}{2}\int_{\mathbb{R}} m_2(\Gamma_\delta * m_2), \tag{1.5}$$

Downloaded from https://www.cambridge.org/core. Lehrst F Alte Geschichte Hist Inst, on 06 Jun 2017 at 07:46:52, subject to the Cambridge Core terms of use, available at https://www.cambridge.org/core/terms. https://doi.org/10.1017/S0956792504005595

where

$$\Gamma_\delta(x) = \frac{1}{4\pi\delta} \log\left(1 + \frac{4\delta^2}{x^2}\right), \tag{1.6}$$

and δ represents the (rescaled) thickness of the sample. Throughout this paper, we consider the functional $F_{q,\delta}$ defined in the set

$$\mathscr{A} = \{\mathbf{m} = (m_1, m_2, m_3) \in H^1(\mathbb{R})^3 || \mathbf{m}| = 1 \text{ a.e., } \mathbf{m} \to \pm\mathbf{e}_3 \text{ as } x \to \pm\infty\}. \tag{1.7}$$

Functional (1.5) was derived by Aharoni [1] by considering equation (1.2) in two dimensions, and carrying out a dimensional reduction. A direct derivation from the three dimensional Landau–Lifshitz model (1.1) is presented in the appendices A through C.

Wall profiles with $m_1 = 0$ are usually called *Bloch walls*, and the profiles with $m_2 = 0$ are called *Néel walls*. These walls constitute the building blocks of more complicated, higher dimensional walls. Only these one-dimensional walls have been found, both numerically and experimentally [19].

The presence of the self-induced field in the energy has a dramatic effect in the structure of the walls. In the case of the Néel wall ($m_2 = 0$), the self-induced field has two opposite effects, giving rise to two different length scales in the wall: it favours a narrow transition layer, and at the same time it favours the existence of a very long tail. The existence of such a long tail is important in the study of the interaction between walls.

This decomposition into a narrow core and a long tail had been observed experimentally, and had been obtained computationally by several authors like Collette [6] and Holz *et al.* [17]. Authors like Aharoni [1] or Dietze & Thomas [12] had tried to determine the wall shape analytically, but their approaches did not produce satisfactory results. In our opinion, one of the best mathematical approaches to the study of this structure was done in 1971 by Riedel & Seeger [21]. However, their paper is unclear in many important details.

The self-induced field also has an important role in the structure of the Bloch wall ($m_1 = 0$). These walls do not have a long tail; the effect of the self-induced field is seen through the presence of oscillations. These oscillations produce the necessary cancellations to lower the energy associated with the wall. To our knowledge, this is the first time that a study of these oscillations has been carried out.

The remainder of the article is organized as follows. In § 2 we study some basic properties of functional (1.5), including lower semicontinuity, existence of minimizers, and asymptotic behaviour. The compactness properties of the functional are analyzed in detail in § 3. The main results of that section is Theorem 3.1, in which we show that if $q = 0$, functional (1.5) has no minimizers.

For the numerical simulations we have implemented a modified Newton's method for energy minimization. Our implementation and the results of our simulations are presented in § 4. In the results one can see the existence of the logarithmic tail for the Néel wall, and the presence of oscillations in the Bloch wall.

In § 5 we present a detailed analysis of the Néel wall. We introduce a related convex functional, whose minimizer can be analyzed in detail. We obtain a description of the Néel wall, and the optimal scaling of the energy functional for Néel walls. In particular, we show that for a given $\delta > 0$,

$$\frac{c_0}{\log \frac{1}{q}} \leqslant \inf_{\mathbf{m} \in \mathscr{A}_n} F^n_{q,\delta}[\mathbf{m}] \leqslant \frac{C_0}{\log \frac{1}{q}} \tag{1.8}$$

Downloaded from https://www.cambridge.org/core. Lehrst F Alte Geschichte Hist Inst, on 06 Jun 2017 at 07:46:52, subject to the Cambridge Core terms of use, available at https://www.cambridge.org/core/terms. https://doi.org/10.1017/S0956792504005595

as $q \to 0$. The results described in § 3 suggest a test function that can be used to obtain the upper bound in (1.8). For the lower bound we use the minimizer of the convex functional introduced in § 5. The limit $\delta \to 0$, $q > 0$ fixed is considered in § 6.

The analysis of the Bloch wall is carried out in § 7. Using the same strategy as in the study of the Néel wall, we obtain a description of the Bloch wall, and the optimal scaling of the energy functional for Bloch walls without anisotropy. In particular, we show that

$$c_0 \delta^{-1/3} \leqslant \inf_{\mathbf{m} \in \mathscr{A}_b} F^b_{0,\delta}[\mathbf{m}] \leqslant C_0 \delta^{-1/3} \tag{1.9}$$

as $\delta \to \infty$, for a Bloch wall.

2 One-dimensional micromagnetic model

We consider the one-dimensional energy functional

$$F_{q,\delta}[\mathbf{m}] = \frac{q}{2} \int_{\mathbb{R}} \left(m_1^2 + m_2^2\right) + \frac{1}{2} \int_{\mathbb{R}} |\mathbf{m}'|^2 + \frac{1}{2} \int_{\mathbb{R}} \left(m_1^2 - m_1(\Gamma_\delta * m_1)\right) + \frac{1}{2} \int_{\mathbb{R}} m_2(\Gamma_\delta * m_2), \tag{2.1}$$

where $q \geqslant 0$, $\delta > 0$, and the function Γ_δ is defined as

$$\Gamma_\delta(x) = \frac{1}{4\pi\delta} \log\left(1 + \frac{4\delta^2}{x^2}\right). \tag{2.2}$$

If we define

$$\Gamma(x) = \frac{1}{2\pi} \log\left(1 + \frac{1}{x^2}\right) \tag{2.3}$$

then

$$\Gamma_\delta(x) = \frac{1}{2\delta} \Gamma\left(\frac{x}{2\delta}\right). \tag{2.4}$$

Note that $\Gamma \in L^1(\mathbb{R}) \cap L^2(\mathbb{R})$, and $\int_{\mathbb{R}} \Gamma(x)\, dx = 1$, so Γ_δ is an approximation to the identity in $\mathbb{R}$. The Fourier transform of Γ_δ is

$$\widehat{\Gamma}_\delta(\xi) = \int_{\mathbb{R}} e^{-2\pi i \xi x} \Gamma_\delta(x)\, dx = \frac{1 - e^{-4\pi\delta|\xi|}}{4\pi\delta|\xi|} \tag{2.5}$$

Using Plancherel's theorem, we can rewrite the convolution terms as

$$\begin{aligned} \int_{\mathbb{R}} m_1^2 - m_1(\Gamma_\delta * m_1)\, dx &= \int_{\mathbb{R}} \widehat{m}_1^2 (1 - \widehat{\Gamma}_\delta(\xi))\, d\xi \\ \int_{\mathbb{R}} m_2\, (\Gamma_\delta * m_2)\, dx &= \int_{\mathbb{R}} \widehat{m}_2^2 \widehat{\Gamma}_\delta(\xi)\, d\xi \end{aligned} \tag{2.6}$$

and therefore, in Fourier space,

$$F_{q,\delta}[\mathbf{m}] = \frac{q}{2} \int_{\mathbb{R}} \left(\widehat{m}_1^2 + \widehat{m}_2^2\right) + \frac{1}{2} \int_{\mathbb{R}} |2\pi\xi \widehat{\mathbf{m}}|^2 + \frac{1}{2} \int_{\mathbb{R}} \left(\widehat{m}_1^2 (1 - \widehat{\Gamma}_\delta) + \widehat{m}_2^2 \widehat{\Gamma}_\delta\right) \tag{2.7}$$

Since $0 \leqslant \widehat{\Gamma}_\delta \leqslant 1$, the functional is nonnegative: $F_\delta[\mathbf{m}] \geqslant 0$.

Downloaded from https://www.cambridge.org/core. Lehrst F Alte Geschichte Hist Inst, on 06 Jun 2017 at 07:46:52, subject to the Cambridge Core terms of use, available at https://www.cambridge.org/core/terms. https://doi.org/10.1017/S0956792504005595

In the following lemmas we study the lower semicontinuity properties of functional (1.5) and show the existence of minimizers.

Lemma 1 *Consider a family of functions* $\{K_h\}_{h>0} \subset L^1(\mathbb{R}^n) \cap L^2(\mathbb{R}^n)$ *such that the family of Fourier transforms* $\{\widehat{K}_h\}_{h>0} \subset L^\infty(\mathbb{R}^n) \cap L^2(\mathbb{R}^n)$ *is uniformly bounded. Assume that*

$$\lim_{h\to 0} \widehat{K}_h(\xi) = \widehat{K}_0(\xi) \quad \text{for almost all } \xi \in \mathbb{R}^n, \tag{2.8}$$

where $\widehat{K}_0 \in L^\infty(\mathbb{R}^n)$. *Then, if* $\{u_h\}_{h>0} \subset L^2(\mathbb{R}^n)$ *converges weakly in* $L^2(\mathbb{R}^2)$ *to* $u_0 \in L^2(\mathbb{R}^n)$ *as* $h \to 0$, *then the family* $\{v_h\}_{h>0} = \{u_h * K_h\}_{h>0}$ *converges weakly in* $L^2(\mathbb{R}^n)$ *to* $v_0 = \mathscr{F}^{-1}(\widehat{u}_0\widehat{K}_0)$, *where we denote by* $\mathscr{F}^{-1}$ *the inverse Fourier transform.*

Proof Let $\phi \in L^2(\mathbb{R}^n)$. Then:

$$\int_{\mathbb{R}^n} v_h\phi = \int_{\mathbb{R}^n} \widehat{v}_h\widehat{\phi} = \int_{\mathbb{R}^n} \widehat{u}_h\widehat{K_h}\widehat{\phi} \tag{2.9}$$

Now, $\{\widehat{K_h}\widehat{\phi}\}_{h>0}$ converges strongly in $L^2(\mathbb{R}^n)$ to $\widehat{K}_0\widehat{\phi}$ as a consequence of the Dominated Convergence Theorem, so the weak convergence of the original family follows easily. □

As a consequence of this lemma, we obtain the weak lower semicontinuity of the one-dimensional energy functional (1.5).

Lemma 2 *Functional* (1.5) *is lower semicontinuous in* $L^2(\mathbb{R})$ *with the weak topology.*

Proof Consider $K_h = \mathscr{F}^{-1}((\widehat{\Gamma}_\delta)^{\frac{1}{2}})$. If a sequence $\{u_h\}$ converges weakly in L^2 to u_0, then $\{u_h * K_h\}_{h>0}$ converges weakly to $u_0 * K_0$, so

$$\begin{aligned}\int_{\mathbb{R}} u_0\,(u_0 * \Gamma_\delta) &= \int_{\mathbb{R}} |\widehat{u}_0|^2\widehat{\Gamma}_\delta = \int_{\mathbb{R}} |u_0 * K_0|^2 \leqslant \liminf_{h\to 0} \int_{\mathbb{R}} |u_h * K_h|^2 \\ &= \liminf_{h\to 0} \int_{\mathbb{R}} |\widehat{u}_h|^2\widehat{\Gamma}_\delta = \liminf_{h\to 0} \int_{\mathbb{R}} u_h\,(u_h * \Gamma_\delta)\end{aligned} \tag{2.10}$$

Considering $K_h = \mathscr{F}^{-1}((1-\widehat{\Gamma}_\delta)^{\frac{1}{2}})$, we obtain that

$$\int_{\mathbb{R}} u_0^2 - \int_{\mathbb{R}} u_0(u_0 * \Gamma_\delta) = \int_{\mathbb{R}} |\widehat{u}_0|^2(1-\widehat{\Gamma}_\delta) \leqslant \liminf_{h\to 0} \left(\int_{\mathbb{R}} u_h^2 - \int_{\mathbb{R}} u_h\,(u_h * \Gamma_\delta)\right) \tag{2.11}$$

□

We can prove now the existence of minimizers.

Lemma 3 *Consider the minimization problem* $\min_{\mathbf{m}\in\mathscr{A}} F_{q,\delta}[\mathbf{m}]$, *where* $F_{q,\delta}[\mathbf{m}]$ *is given by* (1.5), $q > 0$, *and* $\mathscr{A} = \{\mathbf{m} \in H^1(\mathbb{R})^3 | |\mathbf{m}| = 1$ *a.e.,* $\mathbf{m} \to \pm\mathbf{e}_3$ *as* $x \to \pm\infty\}$. *Then,* $\exists\, \mathbf{m}_0 \in \mathscr{A}$ *such that* $F_{q,\delta}[\mathbf{m}_0] = \min_{\mathbf{m}\in\mathscr{A}} F_{q,\delta}[\mathbf{m}]$.

Downloaded from https://www.cambridge.org/core. Lehrst F Alte Geschichte Hist Inst, on 06 Jun 2017 at 07:46:52, subject to the Cambridge Core terms of use, available at https://www.cambridge.org/core/terms. https://doi.org/10.1017/S0956792504005595

Proof Obviously, the set $\mathscr{A}$ is not empty; the vector field $\mathbf{m} = (\cos\theta, 0, \sin\theta)$, where

$$\theta(x) = \begin{cases} -\frac{\pi}{2} & : \quad x < -1 \\ \frac{\pi}{2}x & : \quad x \in [-1, 1] \\ \frac{\pi}{2} & : \quad x > 1 \end{cases}$$

belongs to $\mathscr{A}$.

Let $\alpha = \inf_{\mathbf{m}\in\mathscr{A}} F_{q,\delta}[\mathbf{m}] \geqslant 0$, and consider a minimizing sequence, i.e. $\{\mathbf{m}^j\}_{j\in\mathbb{N}} \in \mathscr{A}$, such that $\lim_{j\to\infty} F_{q,\delta}[\mathbf{m}^j] = \alpha$. Since the energy functional is translation invariant, there is a certain loss of compactness. To avoid this, we impose some extra conditions in our minimizing sequences. Since the function m_3^j changes sign, using a translation if necessary, we can assume that $m_3^j(0) = 0$. Moreover, we can assume that $m_3^j \leqslant 0$ for $x \leqslant 0$, and $m_3^j \geqslant 0$ for $x \geqslant 0$. If that is not the case, we simply need to consider $(m_1^j, m_2^j, sign(x)|m_3^j|)$, which has the same energy as (m_1^j, m_2^j, m_3^j).

Since $q > 0$, there exists a subsequence (not relabeled) such that m_1^j, m_2^j, and $\mathbf{m}^{j\prime}$ converge weakly in $L^2(\mathbb{R})$ to some function $\mathbf{m}_0$. The lower semicontinuity of F with respect to weak convergence in $L^2(\mathbb{R})$ implies that $F_{q,\delta}[\mathbf{m}_0] \leqslant \liminf_j F_{q,\delta}[\mathbf{m}^j] = \alpha$. The Sobolev Embedding Theorem and the Rellich Compactness Theorem imply that $\mathbf{m}^j \in C^0(\mathbb{R})$, the sequence converges uniformly on compact sets, and pointwise on $\mathbb{R}$, so $\mathbf{m}_0 \to \pm\mathbf{e}_3$ as $x \to \pm\infty$, i.e. $\mathbf{m}_0 \in \mathscr{A}$, and therefore $F_{q,\delta}[\mathbf{m}_0] = \alpha > 0$. □

Using Lemma 1 we can determine the limit of the family $\{F_\delta\}_{\delta>0}$, in the sense of Γ-convergence in $\mathscr{A}$, as $\delta \to 0$ and $\delta \to \infty$. The Γ-convergence provides a natural framework for the study of the limiting behaviour of the minimizers of a family of functionals, by identifying these limits as minimizers of a certain limit functional. For our purposes, we only need the following characterization of Γ-convergence [7].

Theorem 2.1 *Let $(X, \mathscr{T})$ be a topological space, and let F_h a family of functionals parameterized by h. A functional F_0 is the Γ-limit of F_h as $h \to 0$ in $\mathscr{T}$ if and only if the two following conditions are satisfied:*

(i) *If $u_h \to u_0$ in $\mathscr{T}$, then $\liminf_{h\to 0} F_h(u_h) \geqslant F_0(u_0)$.*

(ii) *For all $u_0 \in X$, there exists a sequence $u_h \in X$ such that $u_h \to u_0$ in $\mathscr{T}$, and $\lim_{h\to 0} F_h(u_h) = F_0(u_0)$.*

We proceed to identify the Γ-limit of F_δ in $H^1(\mathbb{R})$:

Theorem 2.2 *Consider the functionals*

$$\begin{aligned} F_{q,\infty}[\mathbf{m}] &= \frac{q}{2}\int_{\mathbb{R}} \left(m_1^2 + m_2^2\right) dx + \frac{1}{2}\int_{\mathbb{R}} |\mathbf{m}'|^2\, dx + \frac{1}{2}\int_{\mathbb{R}} m_1^2\, dx \\ F_{q,0}[\mathbf{m}] &= \frac{q}{2}\int_{\mathbb{R}} \left(m_1^2 + m_2^2\right) dx + \frac{1}{2}\int_{\mathbb{R}} |\mathbf{m}'|^2\, dx + \frac{1}{2}\int_{\mathbb{R}} m_2^2\, dx \end{aligned} \tag{2.12}$$

Then $\Gamma - \lim_{\delta\to\infty} F_{q,\delta} = F_{q,\infty}$ and $\Gamma - \lim_{\delta\to 0} F_{q,\delta} = F_{q,0}$, both in the weak topology of $H^1(\mathbb{R})$.

Downloaded from https://www.cambridge.org/core. Lehrst F Alte Geschichte Hist Inst, on 06 Jun 2017 at 07:46:52, subject to the Cambridge Core terms of use, available at https://www.cambridge.org/core/terms. https://doi.org/10.1017/S0956792504005595

Proof We only need to verify that the two conditions (i) and (ii) written above are satisfied. Condition (ii) is trivial, since we can take $\mathbf{m}_\delta = \mathbf{m}$ for all $\delta > 0$, and a simple application of the Dominated Convergence Theorem gives the desired result.

Condition (i) is a direct consequence of Lemma 1, where we studied the behaviour of the functional on weakly convergent sequences. □

As a consequence of the following lemma, if $\mathbf{m}$ minimizes $F_{q,0}$ (resp. $F_{q,\infty}$) in $\mathscr{A}$, then $m_1 = 0$ (resp. $m_2 = 0$).

Lemma 4 *Consider the functional*

$$F[\mathbf{m}] = \frac{\alpha}{2}\int_\Omega m_1^2\,dx + \frac{\beta}{2}\int_\Omega m_2^2\,dx + \frac{\gamma}{2}\int_\Omega |\nabla \mathbf{m}|^2\,dx \tag{2.13}$$

where $\alpha > \beta > 0$, $\gamma > 0$, and $\Omega \subset \mathbb{R}^n$. We consider the problem

$$\min_{\mathbf{m}\in\mathscr{A}} F[\mathbf{m}] \tag{2.14}$$

where $\mathscr{A} \subset H^1(\Omega)^3$ satisfies the following condition:

If $\mathbf{m} = (m_1, m_2, m_3) \in \mathscr{A}$, then $\widetilde{\mathbf{m}} = (0, \sqrt{m_1^2 + m_2^2}, m_3) \in \mathscr{A}$.

Then, if $\mathbf{m}_0$ is a minimizer of the functional in $\mathscr{A}$, it follows that $m_1 = 0$.

Proof The idea of the proof is that if m_1 is not zero, using a rotation, we can obtain a vector field whose first component is identically zero, and that has strictly less energy, so the first component of the minimizer must be identically zero.

Consider the vector field $\widetilde{\mathbf{m}} = (0, \sqrt{m_1^2 + m_2^2}, m_3)$. The energy of this vector field can be easily computed:

$$\begin{aligned}
F[\tilde{\mathbf{m}}] &= \frac{\beta}{2}\int_\Omega m_1^2 + m_2^2\,dx + \frac{\gamma}{2}\int_\Omega \frac{|\nabla m_1|^2 m_1^2 + 2m_1 m_2 \nabla m_1 \nabla m_2 + |\nabla m_2|^2 m_2^2}{m_1^2 + m_2^2} + |\nabla m_3|^2\,dx \\
&= \frac{\beta}{2}\int_\Omega m_1^2 + m_2^2\,dx + \frac{\gamma}{2}\int_\Omega |\nabla \mathbf{m}|^2\,dx - \frac{\gamma}{2}\int_\Omega \frac{|\nabla m_1|^2 m_2^2 - 2m_1 m_2 \nabla m_1 \nabla m_2 + |\nabla m_2|^2 m_1^2}{m_1^2 + m_2^2}\,dx \\
&= \frac{\beta}{2}\int_\Omega m_1^2 + m_2^2\,dx + \frac{\gamma}{2}\int_\Omega |\nabla \mathbf{m}|^2\,dx - \frac{\gamma}{2}\int_\Omega \frac{|m_2 \nabla m_1 - m_1 \nabla m_2|^2}{m_1^2 + m_2^2}\,dx < F[\mathbf{m}]
\end{aligned}$$

Therefore, $m_1 = 0$. □

Functional $F_{q,\infty}$ is precisely the functional used by Landau & Lifshitz [20] for their well-known domain wall computation. The minimizer is

$$\begin{aligned}
\mathbf{m} &= (0, \cos(\theta), \sin(\theta)) \\
\sin(\theta) &= \tanh(\sqrt{q}x)
\end{aligned} \tag{2.15}$$

The transition layer is $O(1/\sqrt{q})$, and the minimum energy is $\inf_{\mathbf{m}\in\mathscr{A}} F_\infty[\mathbf{m}] = 2\sqrt{q}$.

Downloaded from https://www.cambridge.org/core. Lehrst F Alte Geschichte Hist Inst, on 06 Jun 2017 at 07:46:52, subject to the Cambridge Core terms of use, available at https://www.cambridge.org/core/terms. https://doi.org/10.1017/S0956792504005595

Theorem 2.2 and Lemma 4 motivate the following definitions:

$$\begin{aligned} F^n_{q,\delta}[\mathbf{m}] &= \frac{q}{2}\int_{\mathbb{R}} m_1^2 + \frac{1}{2}\int_{\mathbb{R}} |\mathbf{m}'|^2 + \frac{1}{2}\int_{\mathbb{R}} \left(m_1^2 - m_1\,(\Gamma_\delta * m_1)\right) \\ F^b_{q,\delta}[\mathbf{m}] &= \frac{q}{2}\int_{\mathbb{R}} m_2^2 + \frac{1}{2}\int_{\mathbb{R}} |\mathbf{m}'|^2 + \frac{1}{2}\int_{\mathbb{R}} m_2\,(\Gamma_\delta * m_2) \end{aligned} \tag{2.16}$$

and the corresponding spaces $\mathscr{A}_n = \{\mathbf{m} \in \mathscr{A} | m_2 = 0\}$, and $\mathscr{A}_b = \{\mathbf{m} \in \mathscr{A} | m_1 = 0\}$.

Using a calculation analogous to the wall computation performed by Landau & Lifshitz [20], we can obtain the minimum values of $F^n_{q,\delta}$ and $F^b_{q,\delta}$ in the cases $\delta = 0$ and $\delta = \infty$.

(i) $\inf_{\mathbf{m}\in\mathscr{A}_n} F^n_{q,0}[\mathbf{m}] = 2\sqrt{q}$
(ii) $\inf_{\mathbf{m}\in\mathscr{A}_n} F^n_{q,\infty}[\mathbf{m}] = 2\sqrt{q+1}$
(iii) $\inf_{\mathbf{m}\in\mathscr{A}_b} F^b_{q,0}[\mathbf{m}] = 2\sqrt{q+1}$
(iv) $\inf_{\mathbf{m}\in\mathscr{A}_b} F^b_{q,\infty}[\mathbf{m}] = 2\sqrt{q}$

Since the function $\widehat{\Gamma}_\delta$ is a decreasing function of δ, it is clear that for a given $q > 0$, the function $f_q(\delta) = \min_{\mathbf{m}\in\mathscr{A}_n} F^n_{q,\delta}[\mathbf{m}]$ is an increasing function of δ, and the corresponding function for $F^b_{q,\delta}$ is decreasing. As a consequence, there exists a critical δ_c such that, for $\delta < \delta_c$, the Néel wall has less energy than the Bloch wall, and for $\delta > \delta_c$, the Bloch wall has less energy than the Néel wall. For $\delta = \delta_c$, the two energies are the same, and the functional $F_{q,\delta}$ has two different minimizers.

3 Anisotropy and compactness

The condition $q > 0$ is necessary for the existence of minimizers in Lemma 3. We show in Theorem (3.1) that if $q = 0$, functional (1.5) has no minimizers in $\mathscr{A}$. Heuristically, this can be understood as follows: The function m_3 is forced to change from -1 to 1 because of the boundary conditions. The anisotropy energy penalizes the deviations of m_3 from any of these two values, and therefore favours a narrow, or rather non-existing, transition layer. In the absence of anisotropy energy, this transition layer can be made very wide at no expense. The exchange energy penalizes the spatial variations of the magnetization, and therefore favours magnetization distributions that are close to being uniform. The effect of the stray field energy is easier to understand it if we look at the magnetostatic equation:

$$\begin{aligned} \Delta u &= m_{1,x} \\ [u] &= 0 \\ \left[\frac{\partial u}{\partial y}\right] &= m_2 \end{aligned} \tag{3.1}$$

The stray field energy can therefore be reduced if $|m_{1,x}|$ and $|m_2|$ are small, so it again favours distributions that are close to being uniform. The details are contained in the following theorem.

Downloaded from https://www.cambridge.org/core. Lehrst F Alte Geschichte Hist Inst, on 06 Jun 2017 at 07:46:52, subject to the Cambridge Core terms of use, available at https://www.cambridge.org/core/terms. https://doi.org/10.1017/S0956792504005595

Theorem 3.1 *Consider the functional*

$$F_{0,\delta}[\mathbf{m}] = \frac{1}{2}\int_{\mathbb{R}} |\mathbf{m}'|^2\,dx + \frac{1}{2}\int_{\mathbb{R}} \left(m_1^2 - m_1\,(\Gamma_\delta * m_1) + m_2\,(\Gamma_\delta * m_2)\right)\,dx \tag{3.2}$$

where $\mathbf{m} \in \mathscr{A} = \{\mathbf{m} \in H^1(\mathbb{R}) | |\mathbf{m}| = 1, m_3 \to \pm\mathbf{e}_3 \quad as \quad x \to \pm\infty\}$. *Then*

$$\inf_{\mathbf{m}\in\mathscr{A}} F_{0,\delta}[\mathbf{m}] = 0 \tag{3.3}$$

and the infimum is not achieved.

Proof We prove that the infimum is equal to zero. Since the functional is positive, it is clear that that this infimum cannot be achieved in $\mathscr{A}$.

Consider $\mathbf{m} \in \mathscr{A}$ such that $m_2 = 0$. Define $\mathbf{m}_n(x) = \mathbf{m}(\frac{x}{n})$. Then,

$$F_{0,\delta}[\mathbf{m}_n] = \frac{1}{2n}\int_{\mathbb{R}} |\mathbf{m}'|^2\,dy + \frac{1}{2}\int_{\mathbb{R}} |\widehat{m}_1(\xi)|^2 n\left(1 - \widehat{\Gamma}_\delta\left(\frac{\xi}{n}\right)\right)d\xi \tag{3.4}$$

Now,

$$\begin{aligned} n\left(1 - \widehat{\Gamma}_\delta\left(\frac{\xi}{n}\right)\right) &= n\left(1 - \frac{1 - e^{-4\pi\frac{\delta}{n}|\xi|}}{4\pi\frac{\delta}{n}|\xi|}\right) \\ &= n\left(1 - \frac{1 - \left(1 - 4\pi\frac{\delta}{n}|\xi| + \frac{1}{2}\left(4\pi\frac{\delta}{n}|\xi|\right)^2 + O\left(\frac{|\xi|^3}{n^3}\right)\right)}{4\pi\frac{\delta}{n}|\xi|}\right) \\ &= n\left(2\pi\frac{\delta}{n}|\xi| + O\left(\frac{|\xi|^2}{n^2}\right)\right) \overset{n\to\infty}{\longrightarrow} 2\pi\delta|\xi| \end{aligned} \tag{3.5}$$

Therefore

$$\lim_{n\to\infty} F_{0,\delta}[\mathbf{m}_n] = \pi\delta\int_{\mathbb{R}} |\widehat{m}_1(\xi)|^2|\xi|\,d\xi = D[\widehat{m}_1] \tag{3.6}$$

If $\mathbf{m} \in \mathscr{A}$ is a minimizer, then $D[m_1] \geqslant F_{0,\delta}[\mathbf{m}] \geqslant 0$. If we prove that $\inf_{\mathbf{m}\in\mathscr{A}} D[\mathbf{m}] = 0$, it follows that $\inf_{\mathbf{m}\in\mathscr{A}} F_{0,\delta}[\mathbf{m}] = 0$: For any $\epsilon > 0$, we can find a function $\mathbf{m}^\epsilon \in \mathscr{A}$ such that $D[m_1^\epsilon] \leqslant \frac{\epsilon}{2}$. Since $F_{0,\delta}[\mathbf{m}^\epsilon(\frac{x}{n})] \to D[m_1^\epsilon]$, and $\mathbf{m}_n^\epsilon \in \mathscr{A}$, for some n, $F_{0,\delta}[\mathbf{m}_n^\epsilon] < \epsilon$.

We are left with the task of proving that $\inf_{\mathbf{m}\in\mathscr{A}} D[\mathbf{m}] = 0$. Consider the sequence

$$\widehat{u}_n(\xi) = \frac{1}{2\log\frac{1}{a_n}}\frac{1}{|\xi|}\left(\chi_{[-1,-a_n]} + \chi_{[a_n,1]}\right) \tag{3.7}$$

where $a_n \to 0$ as $n \to \infty$. It is easy to verify that

(i) $\int_{\mathbb{R}} \widehat{u}_n = 1$

(ii) $\int_{\mathbb{R}} |\widehat{u}_n| \leqslant 1$

These two conditions imply that $|u_n| \leqslant 1$ and $u_n(0) = 1$. Now,

$$D[\widehat{u}_n] = \frac{\pi\delta}{\left(\log\frac{1}{a_n}\right)^2}\int_{a_n}^1 \frac{1}{|\xi|}\,d\xi = \frac{\pi\delta}{\log\frac{1}{a_n}} \overset{n\to\infty}{\longrightarrow} 0. \tag{3.8}$$

The proof will be complete once we show that $(u_n, 0, \sqrt{1-u_n^2}) \in \mathscr{A}$. The function u_n is smooth and decays fast at infinity, since its Fourier transform is compactly supported. We

Downloaded from https://www.cambridge.org/core. Lehrst F Alte Geschichte Hist Inst, on 06 Jun 2017 at 07:46:52, subject to the Cambridge Core terms of use, available at https://www.cambridge.org/core/terms. https://doi.org/10.1017/S0956792504005595

only need to show that the first derivative of $\sqrt{1-u_n^2}$ belongs to L^2_{loc} in a neighborhood of zero. Later on we will obtain an asymptotic expansion for the function u_n on the whole line, but for now we only need to prove that the function $\sqrt{1-u_n^2}$ is smooth in a neighborhood of zero. Since $\widehat{u}_n$ is an even function, u_n is also even, so $u_n'(0) = 0$. Using a Taylor expansion,

$$\left(\left(\sqrt{1-u_n^2}\right)'\right)^2 = \frac{u_n^2 u_n'^2}{1-u_n^2} \approx \frac{\left(1+\frac{1}{2}u_n''(0)x^2\right)^2 (u_n''(0)x)^2}{1-\left(1+\frac{1}{2}u_n''(0)x^2\right)^2} = -u_n''(0) + O(x), \tag{3.9}$$

and that concludes the proof. □

From the proof of Theorem 3.1, it is clear that when $q = 0$, the Néel functional has no minimizers. This is no longer true for the Bloch wall functional. In a Bloch wall, the stray-field energy acts as a kind of anisotropy. Mathematically we express this in the following inequality.

Lemma 5 *For every $\epsilon > 0$,*

$$\int_{\mathbb{R}} m_2^2\,dx \leqslant \frac{1}{\widehat{\Gamma}_\delta\left(\frac{1}{\epsilon}\right)} \int_{\mathbb{R}} m_2 * \Gamma_\delta m_2\,dx + \epsilon^2 \int_{\mathbb{R}} (m_2')^2\,dx \tag{3.10}$$

Proof Using Plancherel's theorem, and since $\widehat{\Gamma}_\delta(\xi)$ is a decreasing function of ξ, we obtain

$$\int_{\mathbb{R}} m_2^2\,dx = \int_{|\xi|\leqslant\frac{1}{\epsilon}} \widehat{m}_2^2\,d\xi + \int_{|\xi|>\frac{1}{\epsilon}} \widehat{m}_2^2\,d\xi \leqslant \frac{1}{\widehat{\Gamma}_\delta\left(\frac{1}{\epsilon}\right)} \int_{|\xi|\leqslant\frac{1}{\epsilon}} \widehat{m}_2^2 \widehat{\Gamma}_\delta(\xi)\,d\xi + \epsilon^2 \int_{|\xi|>\frac{1}{\epsilon}} \xi^2 \widehat{m}_2^2\,d\xi \tag{3.11}$$

which gives the desired inequality. □

The lack of compactness of the Néel wall functional with no anisotropy is the reason why the Néel wall has a long, logarithmic, tail. The Bloch wall, however, does not have such a long tail; the decay outside the core is rational.

4 One-dimensional walls: numerical analysis

We have implemented a Modified Newton's method with an inexact line search for the minimization of

$$F_{q,\delta}[\mathbf{m}] = \frac{q}{2}\int_{\mathbb{R}} \left(m_1^2 + m_2^2\right) + \frac{1}{2}\int_{\mathbb{R}} |\mathbf{m}'|^2 + \frac{1}{2}\int_{\mathbb{R}} \left(m_1^2 - m_1\left(\Gamma_\delta * m_1\right)\right) + \frac{1}{2}\int_{\mathbb{R}} m_2\left(\Gamma_\delta * m_2\right), \tag{4.1}$$

and the Bloch and Néel wall functionals. In our simulations we have studied the structure of the one dimensional walls, and its dependence on the parameters q and δ.

The properties of the Modified Newton's method are well documented [8], so we will simply describe our implementation.

The real line is truncated to a finite size interval. The results have been compared for several values of the length of the interval, until no change was observed in the main

Downloaded from https://www.cambridge.org/core. Lehrst F Alte Geschichte Hist Inst, on 06 Jun 2017 at 07:46:52, subject to the Cambridge Core terms of use, available at https://www.cambridge.org/core/terms. https://doi.org/10.1017/S0956792504005595

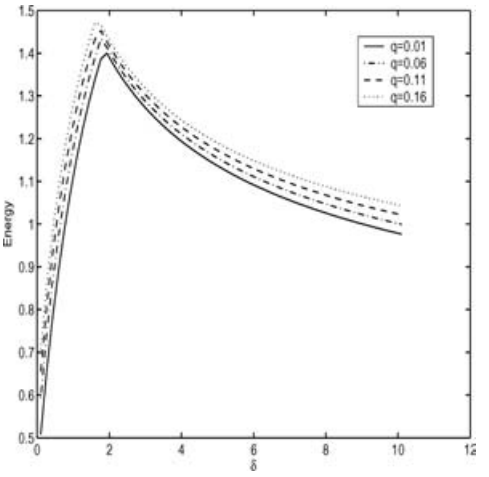

FIGURE 2. Energy profile for different values of q and δ.

characteristics of the wall. For the simulations presented here we considered the interval $[-1000, 1000]$.

In our implementation we have used two different discretizations: The energies are evaluated using a trapezoidal rule with boundary corrections to make it fourth order accurate:

$$\int_{x_0}^{x_n} f(x)\,dx \approx \Delta x \sum_{i=0}^{n} f_i - \frac{\Delta x^2}{12}\left(\frac{3f_n - 4f_{n-1} + f_{n-2}}{2\Delta x} - \frac{f_0 - 4f_1 + 3f_2}{2\Delta x}\right) + O(\Delta x^4). \tag{4.2}$$

The derivatives are computed using standard fourth order finite differences. For the magnetostatic field, we need to compute the following convolution numerically to fourth order accuracy:

$$g(x_k) = \frac{1}{4\pi\delta}\int_0^1 f(y)\,\log\left(1 + \frac{4\delta^2}{(y - x_k)^2}\right) dy. \tag{4.3}$$

We do this by decomposing the integral into a sum of integrals over intervals of length Δx. In each interval, f is approximated using polynomial interpolation, and then the integrals are computed exactly. We have used cubic interpolation for f. The resulting convolution sum is performed with a Fast Fourier Transform (FFT).

The unit length constraint is taken into account by considering the projection of the gradient of the functional onto the tangent plane of the sphere, and by performing the line search on the function

$$f(t) = F\left[\frac{\mathbf{m} + t\mathbf{p}}{|\mathbf{m} + t\mathbf{p}|}\right],$$

where $\mathbf{p}$ is a descent direction, i.e. $f'(0) < 0$.

4.1 Numerical experiments

In our first experiment we minimize functional (1.5) for several values of δ and q. The parameter q ranges in the interval $[0.01, 1.01]$, with increments $\Delta q = 0.05$. The parameter δ ranges in the interval $[.1, 10.]$, with increments $\Delta\delta = 0.05$. Our results, presented in Figure 2,

Downloaded from https://www.cambridge.org/core. Lehrst F Alte Geschichte Hist Inst, on 06 Jun 2017 at 07:46:52, subject to the Cambridge Core terms of use, available at https://www.cambridge.org/core/terms. https://doi.org/10.1017/S0956792504005595

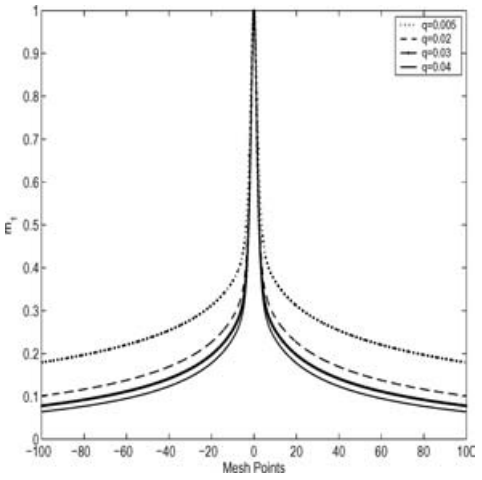

FIGURE 3. Néel wall profile for $\delta = 0.015$; Dependence on the parameter q. Only the interval $[-100, 100]$ is plotted, for clarity.

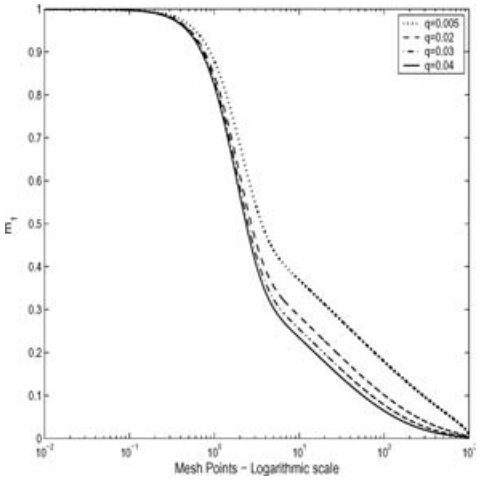

FIGURE 4. Néel wall profile for $\delta = 0.015$; Dependence on the parameter q (Logarithmic scale.)

indicate that functional (1.5) is minimized by a Néel wall for small values of δ, and by a Bloch wall for larger values of δ, consistent with experimental observations. No intermediate structures were found.

In our second experiment, we study the structure of the Néel wall, for small values of q. We use the Néel wall functional, instead of the full one-dimensional micromagnetic functional. The parameter q is fixed, and the functional is minimized for several values of δ. We consider $q \in [0.001, 0.01]$ at intervals $\Delta q = 0.005$.

The results can be seen in Figure 3, where we present the structure of a typical Néel wall. Only the interval $[-100, 100]$ is shown. We only plot the component m_1, since $m_2 = 0$, and $m_3 = \sqrt{1 - m_1^2}$. The dependence of the wall profile on the parameter q may be understood better from Figure 4. In this figure we plot the same results, but the abscissa is plotted

Downloaded from https://www.cambridge.org/core. Lehrst F Alte Geschichte Hist Inst, on 06 Jun 2017 at 07:46:52, subject to the Cambridge Core terms of use, available at https://www.cambridge.org/core/terms. https://doi.org/10.1017/S0956792504005595

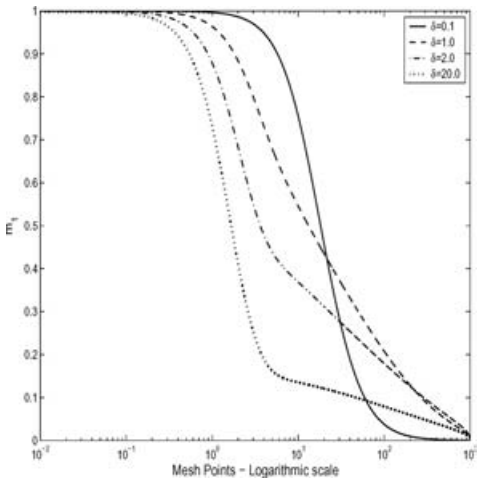

FIGURE 5. Néel wall profile for $q = 0.005$; Dependence on the parameter δ (Logarithmic scale).

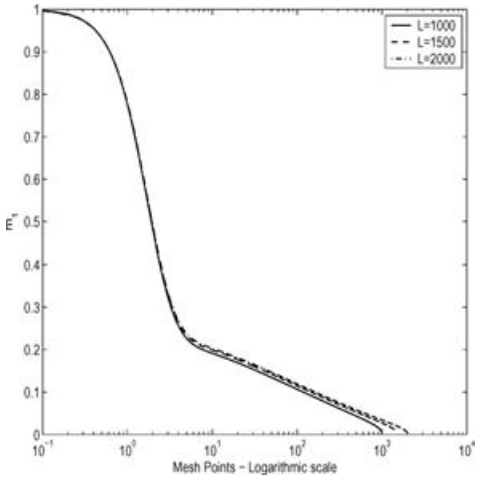

FIGURE 6. Néel wall profile for $q = 0.005$, $\delta = 20$. – Comparison of the wall profiles obtained for different computational intervals.

in logarithmic scale. One of the main characteristics of the Néel wall is the presence of a logarithmic tail. This is evidenced by the existence of a long straight line in the profile. In addition, we observe that there are two different characteristic length scales: the length of the core, and the length of the tail. As the parameter q is increased, both lengths are reduced. This kind of behaviour is expected, since the parameter q is related to the anisotropy.

The dependence of the Néel wall on the parameter δ is shown in Figure 5. The abscissa is plotted in logarithmic scale.

We have studied the dependence of our previous results on the length of the interval considered. In Figure 6 we compare some of these results. Doubling the length of the

Downloaded from https://www.cambridge.org/core. Lehrst F Alte Geschichte Hist Inst, on 06 Jun 2017 at 07:46:52, subject to the Cambridge Core terms of use, available at https://www.cambridge.org/core/terms. https://doi.org/10.1017/S0956792504005595

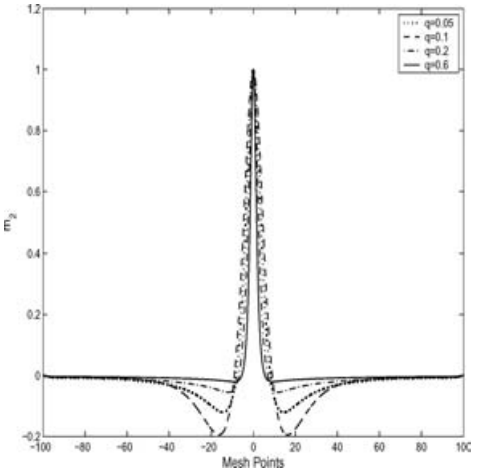

FIGURE 7. Bloch wall profile for $\delta = 100$; Dependence on the parameter q.

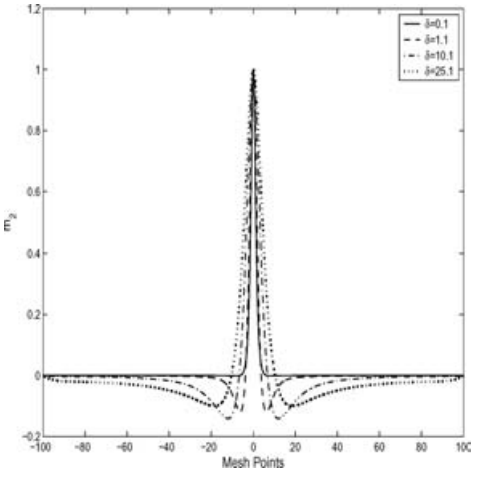

FIGURE 8. Bloch wall profile for $q = 0.045$; Dependence on the parameter δ.

domain does not seem to change the structure of the wall in a significant way, for the parameters considered.

In our last experiments, we have studied the structure of the Bloch wall. In Figure 7 we show the wall structure for several values of the parameter q, and for a fixed value of the parameter δ. We only plot the component m_2, since $m_1 = 0$, and $m_3 = \sqrt{1 - m_2^2}$. The Bloch wall presents oscillations near the core which help reduce the stray field energy. This type of wall does not have a logarithmic tail; it is concentrated in a small region near the origin. The width of the core decreases when q is increased, much like in the Landau–Lifshitz wall structure, equation (2.15).

The dependence of the Bloch wall structure on δ is shown in Figure 8. Since the stray field acts as a kind of anisotropy, which vanishes in the limit $\delta \to 0$, the width of the core increases as δ is increased.

Downloaded from https://www.cambridge.org/core. Lehrst F Alte Geschichte Hist Inst, on 06 Jun 2017 at 07:46:52, subject to the Cambridge Core terms of use, available at https://www.cambridge.org/core/terms. https://doi.org/10.1017/S0956792504005595

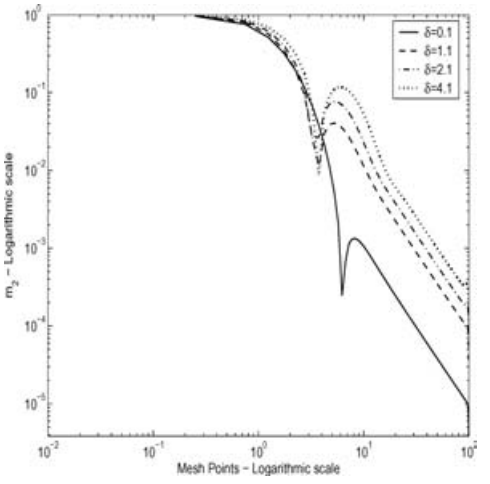

FIGURE 9. Bloch wall profile; Log-log plot.

In our last figure, Figure 9, we show a log − − log plot of the Bloch wall. The decay inside the core is seen to be exponential, and rational outside the core.

5 The Néel Wall

In this section we study the structure of the Néel wall in detail, and in particular the logarithmic tail. We present an asymptotic analysis of the Néel wall as $q \to 0$, and obtain the optimal energy scaling in terms of q. We use the notation $m_1 = g$, $m_2 = 0$, and $m_3 = \text{sign}(x)\sqrt{1-g^2}$. This allows us to write the functional in terms of one function only.

5.1 The lower bound: asymptotic analysis for the Néel Wall

The main difficulties in the analysis of one-dimensional walls are the nonlinear and nonlocal characters of the Euler-Lagrange equation. The nonlinearity appears in the energy functional only through the exchange term:

$$E_e = \frac{1}{2}\int_{\mathbb{R}} \frac{(g')^2}{1-g^2}. \tag{5.1}$$

We consider instead the functional

$$F^l_{q,\delta}[g] = \frac{q}{2}\int_{\mathbb{R}} g^2\,dx + \frac{1}{2}\int_{\mathbb{R}} (g')^2\,dx + \frac{1}{2}\int_{\mathbb{R}} g^2 - g(\Gamma_\delta * g)\,dx. \tag{5.2}$$

By replacing the nonlinearity in the exchange by the condition $g(0) = 1$, we can solve the corresponding Euler-Lagrange equation analytically.

We make a further reduction. The Néel wall is preferred in the thin film limit, so we need only consider the behaviour of the convolution kernel for small frequencies:

Downloaded from https://www.cambridge.org/core. Lehrst F Alte Geschichte Hist Inst, on 06 Jun 2017 at 07:46:52, subject to the Cambridge Core terms of use, available at https://www.cambridge.org/core/terms. https://doi.org/10.1017/S0956792504005595

$1 - \widehat{\Gamma}_\delta(\xi) = 2\pi\delta|\xi| + O(\xi^2)$ for $\delta|\xi| \ll 1$. Hence, we consider the functional

$$\tilde{F}^l_{q,\delta}[g] = \frac{q}{2}\int_{\mathbb{R}} g^2\,dx + \frac{1}{2}\int_{\mathbb{R}} (g')^2\,dx + \frac{2\pi\delta}{2}\int_{\mathbb{R}} |\xi|\widehat{g}^2\,d\xi, \tag{5.3}$$

and the minimization problem

$$\min_{g\in\mathscr{A}} \tilde{F}^l_{q,\delta}[g], \tag{5.4}$$

where

$$\mathscr{A} = \{g \in H^1(\mathbb{R}) | g(0) = 1\}. \tag{5.5}$$

The stray field term has been replaced by the $H^{1/2}(\mathbb{R})$ norm. Note that as a consequence of Hölder's inequality, the energy is still finite for any function $g \in \mathscr{A}$. Later we will see that the difference between $F^l_{q,\delta}$ and $\tilde{F}^l_{q,\delta}$ introduces only high order terms in the energy, leaving the leading order terms unchanged.

The Euler Lagrange equation is

$$qg - g'' + 2\pi\delta\mathscr{F}^{-1}(|\xi|\widehat{g}) = [g']\delta_0, \tag{5.6}$$

where $[g'] = g'(0^+) - g'(0^-)$ and δ_0 is the Dirac distribution concentrated at 0. The equation can be solved using Fourier Transform, and we get:

$$g(x) = 2C\int_0^\infty \frac{\cos(2\pi\xi)}{q + 4\pi^2\xi^2 + 2\pi\delta\xi}\,d\xi, \tag{5.7}$$

where the constant C is determined by the condition that $g(0) = 1$:

$$C = \frac{1}{2\int_0^\infty \frac{1}{q+4\pi^2\xi^2+2\pi\delta\xi}\,d\xi}. \tag{5.8}$$

The denominator in the integrand is a quadratic polynomial, and its roots are

$$\xi_\pm = \frac{-\delta \pm \sqrt{\delta^2 - 4q}}{4\pi}, \tag{5.9}$$

so we can rewrite it as:

$$\frac{1}{q + 4\pi^2\xi^2 + 2\pi\delta\xi} = \frac{1}{4\pi^2(\xi_+ - \xi_-)}\left(\frac{1}{\xi - \xi_+} - \frac{1}{\xi - \xi_-}\right) \tag{5.10}$$

and then the integral is:

$$\begin{aligned} 2\int_0^\infty \frac{1}{q + 4\pi^2\xi^2 + 2\pi\delta\xi}\,d\xi &= \frac{1}{2\pi^2(\xi_+ - \xi_-)}\log\frac{\xi_-}{\xi_+} \\ &= \frac{1}{\pi\sqrt{\delta^2 - 4q}}\log\left(\frac{(\delta + \sqrt{\delta^2 - 4q})^2}{4q}\right) \sim \frac{1}{\pi\delta}\log\frac{\delta}{q}. \end{aligned}$$

Downloaded from https://www.cambridge.org/core. Lehrst F Alte Geschichte Hist Inst, on 06 Jun 2017 at 07:46:52, subject to the Cambridge Core terms of use, available at https://www.cambridge.org/core/terms. https://doi.org/10.1017/S0956792504005595

We can easily compute the minimum energy of $\tilde{F}^l_{q,\delta}$ using its Fourier representation:

$$\min_{g\in\mathscr{A}} \tilde{F}^l_{q,\delta}[q] = C^2 \int_0^\infty \frac{q+4\pi^2\xi^2+2\delta\xi}{(q+4\pi^2\xi^2+2\delta\xi)^2}\,d\xi = C^2\int_0^\infty \frac{1}{q+4\pi^2\xi^2+2\delta\xi}\,d\xi$$
$$= C^2\frac{1}{2C} = \frac{C}{2} = \pi\sqrt{\delta^2-4q}\,\frac{1}{\log\left(\frac{(\delta+\sqrt{\delta^2-4q})^2}{4q}\right)} = \frac{\pi\delta}{\log\frac{\delta}{q}} + o\left(\frac{1}{\log\frac{1}{q}}\right).$$

This provides us with a lower bound for the original (non convex) energy functional once we notice that

$$\int_{\mathbb{R}} \frac{(g')^2}{1-g^2}\,dx \geqslant \int_{\mathbb{R}} (g')^2\,dx \tag{5.11}$$

and

$$\int_{\mathbb{R}} \frac{1}{q+4\pi^2\xi^2+1-\widehat{\Gamma}_\delta(\xi)}\,d\xi$$
$$= \int_{\mathbb{R}} \frac{1}{q+4\pi^2\xi^2+2\pi\delta|\xi|}\,d\xi + \int_{\mathbb{R}} \left(\frac{1}{q+4\pi^2\xi^2+1-\widehat{\Gamma}_\delta(\xi)} - \frac{1}{q+4\pi^2\xi^2+2\pi\delta|\xi|}\right)d\xi$$
$$= \int_{\mathbb{R}} \frac{1}{q+4\pi^2\xi^2+2\pi\delta|\xi|}\,d\xi + \int_{\mathbb{R}} \frac{2\pi\delta|\xi|-1+\widehat{\Gamma}_\delta(\xi)}{(q+4\pi^2\xi^2+2\pi\delta|\xi|)(q+4\pi^2\xi^2+1-\widehat{\Gamma}_\delta(\xi))}\,d\xi. \tag{5.12}$$

It is easy to show that $2\pi\delta|\xi|-1+\widehat{\Gamma}_\delta(\xi)>0$ for all $\xi\in\mathbb{R}$. Therefore,

$$\frac{c_0}{\log\frac{1}{q}} \leqslant \min_g \tilde{F}^l_{q,\delta}[g] \leqslant \min_g F_{q,\delta}[g]. \tag{5.13}$$

Now we proceed with the asymptotic analysis. In order to simplify the expressions, we only use the leading order terms in the expressions for ξ_+, ξ_-, and C. Since we are studying the asymptotic behaviour of the minimizers as $q\to 0$, for a fixed δ, we simply assume $\delta=1$, which will make the presentation more clear. Hence, we consider:

$$\xi_+ = -\frac{q}{2\pi}$$
$$\xi_- = -\frac{1-q}{2\pi}$$
$$C = 2\pi\frac{1}{\log\frac{1}{q}}.$$

We use the decomposition of the denominator and obtain:

$$g(x) = \frac{C}{2\pi^2}\frac{1}{\xi_+-\xi_-}\int_0^\infty \cos(2\pi\xi x)\left(\frac{1}{\xi-\xi_+}-\frac{1}{\xi-\xi_-}\right)d\xi. \tag{5.14}$$

Downloaded from https://www.cambridge.org/core. Lehrst F Alte Geschichte Hist Inst, on 06 Jun 2017 at 07:46:52, subject to the Cambridge Core terms of use, available at https://www.cambridge.org/core/terms. https://doi.org/10.1017/S0956792504005595

Substituting the values of ξ_+, ξ_-, and C:

$$\begin{aligned} g(x) &= \frac{1}{\log\frac{1}{q}}\int_0^\infty \cos(2\pi\xi x)\left(\frac{1}{\xi+\frac{q}{2\pi}}-\frac{1}{\xi+\frac{1-q}{2\pi}}\right)d\xi \\ &= \frac{1}{\log\frac{1}{q}}\left(\cos(xq)\int_{xq}^\infty \frac{\cos t}{t}\,dt+\sin(xq)\int_{xq}^\infty \frac{\sin t}{t}\,dt\right. \\ &\quad \left.-\cos(x(1-q))\int_{x(1-q)}^\infty \frac{\cos t}{t}\,dt-\sin(x(1-q))\int_{x(1-q)}^\infty \frac{\sin t}{t}\,dt\right) \\ &= \frac{1}{\log\frac{1}{q}}(\cos(xq)\,Ci(xq)+\sin(xq)\,si(xq)-\cos(x(1-q))\,Ci(x(1-q)) \\ &\quad -\sin(x(1-q))\,si(x(1-q))), \end{aligned} \tag{5.15}$$

where $Ci(x)$ and $si(x)$ are the Cosine and Sine integrals. The asymptotic representation of these functions is well known [2]:

$$\begin{aligned} Ci(z) &= \int_z^\infty \frac{\cos t}{t}\,dt = -\gamma+\log\frac{1}{z}-\sum_{n=1}^\infty \frac{(-1)^n}{2n(2n)!}z^{2n} \quad \text{for } z \text{ bounded} \\ Ci(z) &\sim -\frac{\sin z}{z}+\frac{\cos z}{z^2}+2\frac{\sin z}{z^3}+O\left(\frac{1}{z^4}\right) \quad \text{for } |z|\gg 1 \\ si(z) &= \frac{\pi}{2}-\sum_{n=0}^\infty \frac{(-1)^n}{(2n+1)(2n+1)!}z^{2n+1} \quad \text{for } z \text{ bounded} \\ si(z) &\sim \frac{\cos z}{z}+\frac{\sin z}{z^2}-2\frac{\cos z}{z^3}+O\left(\frac{1}{z^4}\right) \quad \text{for } |z|\gg 1 \end{aligned} \tag{5.16}$$

where $\gamma = 0.557721\ldots$ is Euler's constant.

Substituting in the expression for the function g, we obtain the following behaviour:

$$\begin{aligned} g(x) &\sim 1-\frac{\pi}{\log\frac{1}{q}}x \quad \text{for } |x|\ll 1 \\ g(x) &\sim -\gamma\frac{1}{\log\frac{1}{q}}+\frac{1}{\log\frac{1}{q}}\log\frac{1}{qx}+O\left(\frac{\pi qx}{2\log\frac{1}{q}}\right) \quad \text{for } 1\ll|x|\ll\frac{1}{q} \\ g(x) &\sim \frac{1}{\log\frac{1}{q}}\frac{1}{x^2q^2}+\frac{1}{\log\frac{1}{q}}\frac{1}{x^2}+O\left(\frac{1}{x^4}\frac{1}{\log\frac{1}{q}}\right) \quad \text{for } \frac{1}{q}\ll|x|. \end{aligned} \tag{5.17}$$

This expression shows the logarithmic tail, and the rational decay.

In Figure 10 we compare the profile of the Néel wall computed with the energy minimization algorithm described in section 4, and the profile obtained by evaluating the inverse Fourier transform (5.7). The Fourier Transform was computed using a Hurwitz–Zweifel expansion, combined with a Clenshaw–Curtis quadrature [22]. The parameters used are $L = 4000$, $\delta = 20$, and $q = 0.005$. This plot shows how the significant length

Downloaded from https://www.cambridge.org/core. Lehrst F Alte Geschichte Hist Inst, on 06 Jun 2017 at 07:46:52, subject to the Cambridge Core terms of use, available at https://www.cambridge.org/core/terms. https://doi.org/10.1017/S0956792504005595

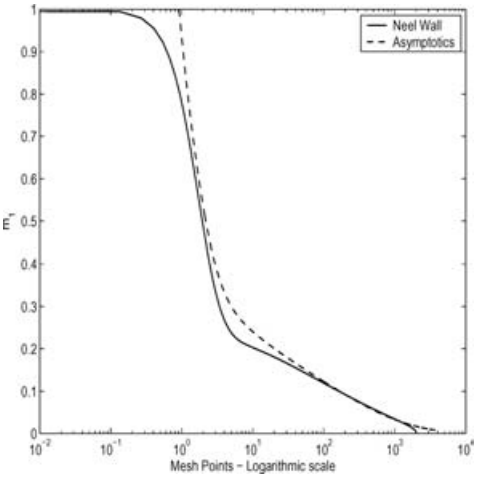

FIGURE 10. Comparison of the Néel wall profile obtained with our energy minimization algorithm and the approximation obtained via Fourier transform. The parameters used are $L = 4000$, $\delta = 20$, and $q = 0.005$.

scales (core and tail length) are captured reliably by our asymptotic approximation, even though the details of the profile in the core and in the tail are not too accurate.

5.2 The upper bound

We use the profile used to prove the lack of minimizers in the case $q = 0$, theorem 3.1, to obtain a matching upper bound. Consider

$$\widehat{g}(\xi) = \frac{1}{2\log\frac{1}{q}}\frac{1}{|\xi|}\left(\chi_{[-1,-q]} + \chi_{[q,1]}\right). \tag{5.18}$$

Then

$$g(x) = \frac{1}{\log\frac{1}{q}}\int_q^1 \frac{\cos(2\pi\xi x)}{\xi}\,d\xi = \frac{1}{\log\frac{1}{q}}\int_{2\pi xq}^{2\pi x}\frac{\cos t}{t}\,dt = \frac{1}{\log\frac{1}{q}}(Ci(2\pi xq) - Ci(2\pi x)). \tag{5.19}$$

As before, we study the behaviour of this function:

$$\begin{aligned}
g(x) &\sim 1 - \frac{\pi^2 x^2}{\log\frac{1}{q}} + O\left(x^4\frac{1}{\log\frac{1}{q}}\right) \quad \text{for } x \ll 1\\
g(x) &\sim 1 - \frac{\gamma}{\log\frac{1}{q}} + \frac{1}{\log\frac{1}{q}}\log\frac{1}{2\pi x} + O\left(\frac{q^2}{\log\frac{1}{q}}x^2\right) \quad \text{for } 1 \ll x \ll \frac{1}{q}\\
g(x) &\sim -\frac{1}{\log\frac{1}{q}}\frac{\sin(2\pi xq)}{2\pi xq} + O\left(\frac{1}{\log\frac{1}{q}}\frac{\sin x}{x}\right) \quad \text{for } \frac{1}{q} \ll x.
\end{aligned} \tag{5.20}$$

Downloaded from https://www.cambridge.org/core. Lehrst F Alte Geschichte Hist Inst, on 06 Jun 2017 at 07:46:52, subject to the Cambridge Core terms of use, available at https://www.cambridge.org/core/terms. https://doi.org/10.1017/S0956792504005595

Now we can estimate the energy:

$$
\begin{aligned}
E_a &= \frac{q}{2}\int_{\mathbb{R}} g^2 = \frac{q}{4\log^2\frac{1}{q}}\int_q^1 \frac{1}{\xi^2}\,d\xi = \frac{1-q}{4\log^2\frac{1}{q}},\\
E_s &= \frac{1}{2}\int_{\mathbb{R}} g^2 - g * \Gamma_1 g = \frac{1}{4\log^2\frac{1}{q}}\int_q^1 \frac{1}{\xi^2}(1-\widehat{\Gamma}_1(\xi))\,d\xi\\
&= \frac{1}{4\log^2\frac{1}{q}}\sum_{n=2}^{\infty}\frac{(-1)^n}{n!}(4\pi)^{n-1}\int_q^1 \xi^{n-3}\,d\xi\\
&= \frac{1}{4\log^2\frac{1}{q}}\left(2\pi\log\frac{1}{q} + \sum_{n=3}^{\infty}\frac{(-1)^n}{(n-2)n!}(4\pi)^{n-1}(1-q^{n-2})\right) \sim \frac{\pi}{2\log\frac{1}{q}} + O\left(\frac{1}{\log^2\frac{1}{q}}\right).
\end{aligned}
$$

To evaluate the exchange energy, we need to estimate the function $h(x) = \sqrt{1-g^2}$:

$$
\begin{aligned}
h(x) &\sim \frac{\sqrt{2}\pi}{\sqrt{\log\frac{1}{q}}}x \quad \text{for } x \ll 1\\
h(x) &\sim \frac{\sqrt{2\gamma}}{\sqrt{\log\frac{1}{q}}}\left(1 - \frac{1}{2\gamma}\log\frac{1}{2\pi x}\right) \quad \text{for } 1 \ll x \ll \frac{1}{q}\\
h(x) &\sim 1 - \frac{1}{2\log^2\frac{1}{q}}\frac{\sin^2(2\pi q x)}{(2\pi q x)^2} \quad \text{for } \frac{1}{q} \ll x.
\end{aligned}
\tag{5.21}
$$

Now we estimate the exchange energy:

$$
\begin{aligned}
E_{ex} &= \frac{1}{2}\int_{\mathbb{R}} (g')^2 + (h')^2\,dx = \frac{1}{4\log^2\frac{1}{q}}\int_q^1 \frac{4\pi^2\xi^2}{\xi^2}\,d\xi + \frac{1}{2}\int_{\mathbb{R}}(h')^2\,dx\\
&= \frac{\pi^2(1-q)}{\log^2\frac{1}{q}} + \frac{1}{2}\int_{\mathbb{R}}(h')^2\,dx.
\end{aligned}
\tag{5.22}
$$

Substituting the asymptotic expression for h and integrating, we get:

$$
E_{ex} = \frac{\pi^2(1-q)}{\log^2\frac{1}{q}} + \frac{2\pi^2}{\log\frac{1}{q}} + \frac{1-q}{4\gamma\log\frac{1}{q}} + \frac{q}{4\log^4\frac{1}{q}}.
\tag{5.23}
$$

Therefore, the energy can be bounded by

$$
F_{q,\delta}[g] \leqslant \frac{C_0}{\log\frac{1}{q}}.
\tag{5.24}
$$

We summarize these results in the following.

Theorem 5.1 *Consider the Néel wall functional*

$$
F^n_{q,\delta}[\mathbf{m}] = \frac{q}{2}\int_{\mathbb{R}} m_1^2 + \frac{1}{2}\int_{\mathbb{R}} |\mathbf{m}'|^2 + \frac{1}{2}\int_{\mathbb{R}}\left(m_1^2 - m_1(\Gamma_\delta * m_1)\right),
$$

Downloaded from https://www.cambridge.org/core. Lehrst F Alte Geschichte Hist Inst, on 06 Jun 2017 at 07:46:52, subject to the Cambridge Core terms of use, available at https://www.cambridge.org/core/terms. https://doi.org/10.1017/S0956792504005595

and $\mathscr{A}_n = \{\mathbf{m} \in \mathscr{A} |\ m_2 = 0\}$. *Given* $\delta > 0$ *fixed, there exist* (*nonnegative*) *constants* c_0 *and* C_0 *such that*

$$\frac{c_0}{\log \frac{1}{q}} \leqslant \min_{\mathbf{m}\in\mathscr{A}_n} F^n_{q,\delta}[\mathbf{m}] \leqslant \frac{C_0}{\log \frac{1}{q}}. \tag{5.25}$$

6 The Néel Wall in the thin film limit: $\delta \to 0$

In this section we study the structure of the Néel wall in the limit $\delta \to 0$, for a fixed value of $q > 0$. The optimal energy for this case was obtained in § 2 in connection with the Γ-limit of functional 1.5. In fact, one can show that

$$\inf_{\mathbf{m}\in\mathscr{A}_n} F^n_{q,\delta}[\mathbf{m}] = 2\sqrt{q} + O(\delta) \tag{6.1}$$

as $\delta \to 0$, which follows from the fact that $1 - \widehat{\Gamma}_\delta(\xi) \leqslant 2\pi\delta|\xi|$ for all $\xi \in \mathbb{R}$, which implies the interpolation inequality

$$\int_{\mathbb{R}} (1 - \widehat{\Gamma}(\xi))\widehat{m}_1^2\, d\xi \leqslant \frac{\delta}{2}\int_{\mathbb{R}} \widehat{m}_1^2 + 4\pi^2\xi^2\widehat{m}_1^2\, d\xi = \frac{\delta}{2}\int_{\mathbb{R}} m_1^2 + (m_1')^2\, dx. \tag{6.2}$$

To study the structure of the Néel wall in this case, we consider the following convex functional:

$$F[g] = \frac{q}{2}\int_{\mathbb{R}} g^2\, dx + \frac{1}{2}\int_{\mathbb{R}} (g')^2\, dx + \frac{1}{2}\int_{\mathbb{R}} 2\pi\delta|\xi||\hat{g}|^2\, d\xi, \tag{6.3}$$

defined on

$$\mathscr{A} = \left\{g \in H^1(\mathbb{R}) | g(0) = 1\right\}. \tag{6.4}$$

We proceed as in the previous section. The Euler-Lagrange equation, in Fourier space, is

$$\hat{g}(\xi)(q + 4\pi^2\xi^2 + 2\pi|\xi|) = C.$$

The solution is

$$g(x) = 2C\int_0^\infty \frac{\cos(2\pi\xi x)}{q + 4\pi^2\xi^2 + 2\pi\delta\xi}\, d\xi = \frac{C}{\pi}\int_0^\infty \frac{\cos(\xi x)}{q + \xi^2 + \delta\xi}\, d\xi.$$

We write

$$q + \xi^2 + \delta\xi = \left(\xi + \frac{\delta}{2}\right)^2 + q - \frac{\delta^2}{4}$$

so

$$g(x) = \frac{C}{\pi\sqrt{q - \delta^2/4}}\int_0^\infty \frac{\cos(\xi x)}{1 + \left(\frac{\xi + \delta/2}{\sqrt{q - \delta^2/4}}\right)^2}\frac{d\xi}{\sqrt{q - \delta^2/4}}.$$

After the change of variables

$$\eta = \frac{\xi + \delta/2}{\sqrt{q - \delta^2/4}}$$

we obtain

$$g(x) = \frac{C}{\pi\sqrt{q - \delta^2/4}}\int_{\frac{\delta/2}{\sqrt{q-\delta^2/4}}}^\infty \frac{\cos(\eta\sqrt{q - \delta^2/4}\, x - \delta x/2)}{\eta^2 + 1}\, d\eta.$$

Downloaded from https://www.cambridge.org/core. Lehrst F Alte Geschichte Hist Inst, on 06 Jun 2017 at 07:46:52, subject to the Cambridge Core terms of use, available at https://www.cambridge.org/core/terms. https://doi.org/10.1017/S0956792504005595

Define $y = \sqrt{q-\delta^2/4}\,x$. We write

$$g(x) = \frac{C}{\pi\sqrt{q-\delta^2/4}}\left(\cos(\delta x/2)\int_{\frac{\delta/2}{\sqrt{q-\delta^2/4}}}^{\infty}\frac{\cos(\eta y)}{\eta^2+1}\,d\eta + \sin(\delta x/2)\int_{\frac{\delta/2}{\sqrt{q-\delta^2/4}}}^{\infty}\frac{\sin(\eta y)}{\eta^2+1}\,d\eta\right).$$

The constant C can be evaluated imposing that $g(0) = 1$:

$$C = \frac{\pi\sqrt{q-\delta^2/4}}{\frac{\pi}{2} - \tan^{-1}\left(\frac{\delta/2}{\sqrt{q-\delta^2 4}}\right)} \sim 2\sqrt{q} + \frac{2}{\pi}\delta - \frac{1}{4}\frac{\pi^2-8}{\pi^2\sqrt{q}}\delta^2 - \frac{1}{6}\frac{\pi^2-12}{\pi^3 q}\delta^3 + O(\delta^4).$$

The minimum energy can be computed directly from C:

$$\min_{g\in\mathscr{A}} F[g] = \frac{C}{2} \sim \sqrt{q} + O(\delta). \tag{6.5}$$

We know that the optimal energy for functional 1.5 in the limit $\delta \to 0$ is $2\sqrt{q}$. Therefore, we do not expect convergence of our asymptotic approximation to the actual minimizer of 1.5 in $H^1(\mathbb{R})$.

Now we estimate each term. Firstly,

$$\int_{\frac{\delta/2}{\sqrt{q-\delta^2/4}}}^{\infty}\frac{\cos(\eta y)}{\eta^2+1}\,d\eta = \int_0^{\infty}\frac{\cos(\eta y)}{\eta^2+1}\,d\eta - \int_0^{\frac{\delta/2}{\sqrt{q-\delta^2/4}}}\frac{\cos(\eta y)}{\eta^2+1}\,d\eta = \frac{\pi}{2}e^{-|y|} - \int_0^{\frac{\delta/2}{\sqrt{q-\delta^2/4}}}\frac{\cos(\eta y)}{\eta^2+1}\,d\eta. \tag{6.6}$$

Now if $\frac{\delta/2}{\sqrt{q-\delta^2/4}}y \ll 1$, or, equivalently, $\delta x \ll 1$, then

$$\begin{aligned}\int_0^{\frac{\delta/2}{\sqrt{q-\delta^2/4}}}\frac{\cos(\eta y)}{\eta^2+1}\,d\eta &= \sum_{n=0}^{\infty}(-1)^n\frac{y^{2n}}{(2n)!}\int_0^{\frac{\delta/2}{\sqrt{q-\delta^2/4}}}\frac{\eta^{2n}}{1+\eta^2}\,d\eta \\ &\sim \arctan\left(\frac{\delta/2}{\sqrt{q-\delta^2/4}}\right) - \frac{y^2}{2}O(\delta^3).\end{aligned} \tag{6.7}$$

If $\delta x \gg 1$ then we can integrate by parts:

$$\int_0^{\frac{\delta}{\sqrt{q-\delta}}}\frac{\cos(\eta y)}{\eta^2+1}\,d\eta = \frac{1}{y}\frac{\sin(\delta x)}{1+\frac{\delta^2}{q-\delta^2}} - \frac{2\delta}{y^2\sqrt{q-\delta^2}}\frac{\cos(\delta x)}{\left(1+\frac{\delta^2}{q-\delta^2}\right)^2} + O\left(\frac{1}{y^3}\right).$$

Now the next term:

$$\int_{\frac{\delta}{\sqrt{q-\delta}}}^{\infty}\frac{\sin(\eta y)}{\eta^2+1}\,d\eta = \int_0^{\infty}\frac{\sin(\eta y)}{\eta^2+1}\,d\eta - \int_0^{\frac{\delta}{\sqrt{q-\delta^2}}}\frac{\sin(\eta y)}{\eta^2+1}\,d\eta.$$

Using residues, the first term can be written as

$$\int_0^{\infty}\frac{\sin(\eta y)}{1+\eta^2}\,d\eta = \frac{1}{2}\{e^y Ei(y) - e^{-y}\bar{E}i(y)\}, \tag{6.8}$$

Downloaded from https://www.cambridge.org/core. Lehrst F Alte Geschichte Hist Inst, on 06 Jun 2017 at 07:46:52, subject to the Cambridge Core terms of use, available at https://www.cambridge.org/core/terms. https://doi.org/10.1017/S0956792504005595

where Ei and $\bar{E}i$ are called exponential integrals, and are defined as

$$Ei(y) = \int_y^\infty \frac{e^{-t}}{t}\,dt,\ \bar{E}i(y) = \fint_{-y}^\infty \frac{e^{-t}}{t}\,dt \quad \text{(Principal Value)}. \tag{6.9}$$

We consider now the following representations for the exponential integrals for $y \ll 1$:

$$Ei(y) = -\gamma - \log(y) - \sum_{n=1}^\infty \frac{(-1)^n}{n\cdot n!} y^n$$
$$\bar{E}i(y) = -\gamma - \log(y) - \sum_{n=1}^\infty \frac{1}{n\cdot n!} y^n,$$

and for $y \gg 1$:

$$Ei(y) = \frac{e^{-y}}{y} - \frac{e^{-y}}{y^2} + 2\frac{e^{-y}}{y^3} + O\left(\frac{e^{-y}}{y^4}\right)$$
$$\bar{E}i(y) = -\frac{e^{y}}{y} - \frac{e^{y}}{y^2} - 2\frac{e^{y}}{y^3} + O\left(\frac{e^{y}}{y^4}\right).$$

Putting these two things together we obtain

$$\int_0^\infty \frac{\sin(\eta y)}{1+\eta^2}\,d\eta = -\sinh(y)\log(y) - \gamma\sinh(y) - \sinh(y)\sum_{n=1}^\infty \frac{y^{2n}}{2n\cdot(2n)!}$$
$$+\cosh(y)\sum_{n=1}^\infty \frac{y^{2n-1}}{(2n-1)\cdot(2n-1)!} = -y\log(y) + (1-\gamma)y - \frac{y^3}{6}\log(y)$$
$$-\left(\frac{\gamma}{6} + \frac{1}{4} - \frac{1}{3\cdot 3!} - \frac{1}{2}\right)y^3 - \frac{y^5}{5!}\log(y)$$
$$-\left(\frac{\gamma}{5!} + \frac{1}{4\cdot 4!} + \frac{1}{4\cdot 3!} - \frac{1}{5\cdot 5!} - \frac{1}{3\cdot 3!} - \frac{1}{4!}\right)y^5 + O(y^7\log(y)),$$

for $y \ll 1$ and

$$\int_0^\infty \frac{\sin(\eta y)}{1+\eta^2}\,d\eta = \frac{1}{y} + \frac{2}{y^3} + O\left(\frac{1}{y^5}\right),$$

for $y \gg 1$.

Now we consider the term

$$\int_0^{\frac{\delta/2}{\sqrt{q-\delta^2/4}}} \frac{\sin(\eta y)}{\eta^2+1}\,d\eta.$$

If $y \ll 1$,

$$\int_0^{\frac{\delta/2}{\sqrt{q-\delta^2/4}}} \frac{\sin(\eta y)}{\eta^2+1}\,d\eta = \sum_{n=0}^\infty \frac{(-1)^n}{(2n+1)!} y^{2n+1} \int_0^{\frac{\delta/2}{\sqrt{q-\delta^2/4}}} \frac{\eta^{2n+1}}{\eta^2+1}\,d\eta$$
$$\sim \frac{1}{2}\log\left(1 + \frac{\delta^2/4}{q-\delta^2/4}\right) y + y^3 O(\delta^4) \tag{6.10}$$

Downloaded from https://www.cambridge.org/core. Lehrst F Alte Geschichte Hist Inst, on 06 Jun 2017 at 07:46:52, subject to the Cambridge Core terms of use, available at https://www.cambridge.org/core/terms. https://doi.org/10.1017/S0956792504005595

and if $y \gg 1$,

$$\int_0^{\frac{\delta/2}{\sqrt{q-\delta^2/4}}} \frac{\sin(\eta y)}{\eta^2+1}\, d\eta \sim \frac{1}{y}\left(1-\frac{\cos(\frac{\delta x}{2})}{1+\frac{\delta^2/4}{q-\delta^2/4}}\right)-\frac{1}{y^2}\sin\left(\frac{\delta x}{2}\right)\frac{\delta}{\sqrt{q-\delta^2/4}}\frac{1}{\left(1+\frac{\delta^2/4}{q-\delta^2/4}\right)^2}+O\left(\frac{1}{y^3}\right). \tag{6.11}$$

From all this, we can obtain the behaviour of the minimizer in the different regimes:

$$g(x) \sim 1-\sqrt{q}x+\frac{1}{2}qx^2-\frac{1}{2}\frac{x(2\,xq\,\ln(\sqrt{q}x)-3\,q\,x+2\,xq\,\gamma+2\sqrt{q})}{\pi\sqrt{q}}\delta+O(\delta^2) \quad \text{for } x \ll \frac{1}{\sqrt{q}}$$

$$g(x) \sim e^{-\sqrt{q}x}+\frac{\left(2+q\,e^{-\sqrt{q}x}x^2\right)}{\pi x^2 q^{\frac{3}{2}}}\delta+O(\delta^2) \quad \text{for } \frac{1}{\sqrt{q}} \ll x \ll \frac{1}{\delta}$$

$$g(x) \sim 2\,\frac{1}{q^{3/2}\pi\,x^2}\delta+O\left(\frac{\delta^2}{x^4}\right) \quad \text{for } \frac{1}{\delta} \ll x.$$

7 The Bloch Wall

In this section we study the case $q = 0$, $\delta \to \infty$ using the same techniques that we used for the study of Néel walls. This will allow us to understand the structure of the wall.

7.1 The lower bound

Lemma 5 allows us to obtain a lower bound for the Bloch wall energy functional, and some insight on the length scales in the problem. By Lemma 5, we find the following inequality:

$$F^b_{0,\delta}[\mathbf{m}] \geqslant \frac{1}{2}\int_{\mathbb{R}} |\mathbf{m}'|^2\, dx - \frac{\epsilon^2\widehat{\Gamma}_\delta\left(\frac{1}{\epsilon}\right)}{2}\int_{\mathbb{R}}(m_2')^2\, dx + \frac{\widehat{\Gamma}_\delta\left(\frac{1}{\epsilon}\right)}{2}\int_{\mathbb{R}} m_2^2\, dx. \tag{7.1}$$

Now, we choose ϵ such that

$$\epsilon^2\widehat{\Gamma}_\delta\left(\frac{1}{\epsilon}\right) = \frac{1}{4}, \tag{7.2}$$

and therefore

$$F^b_{0,\delta}[\mathbf{m}] \geqslant \frac{1}{4}\int_{\mathbb{R}} |\mathbf{m}'|^2\, dx + \frac{1}{2\epsilon^2}\int_{\mathbb{R}} m_2^2\, dx. \tag{7.3}$$

We have already computed the minimum energy of the functional on the right-hand side, and so

$$F^b_{0,\delta}[\mathbf{m}] \geqslant \frac{\sqrt{2}}{2\epsilon}. \tag{7.4}$$

Now, since

$$\epsilon^2\widehat{\Gamma}_\delta\left(\frac{1}{\epsilon}\right) = \frac{1}{4}. \tag{7.5}$$

we obtain that

$$\epsilon^3\frac{1-e^{-4\pi\delta/\epsilon}}{4\pi\delta} = \frac{1}{4}. \tag{7.6}$$

Downloaded from https://www.cambridge.org/core. Lehrst F Alte Geschichte Hist Inst, on 06 Jun 2017 at 07:46:52, subject to the Cambridge Core terms of use, available at https://www.cambridge.org/core/terms. https://doi.org/10.1017/S0956792504005595

and so

$$\frac{\epsilon^3}{4\pi\delta} \sim \frac{1}{4}, \tag{7.7}$$

which ultimately implies $\epsilon \sim \delta^{1/3}$. Hence

$$\min_{\mathbf{m}\in\mathscr{A}_b} F^b_{0,\delta}[\mathbf{m}] \geqslant c_0\delta^{-1/3}. \tag{7.8}$$

7.2 The upper bound

We can match this lower bound with an upper bound that has the same scaling in δ. To do this, consider a smooth, even, nonnegative function $\widehat{\phi}$ such that $\widehat{\phi}(0) = 0$, $\int_{\mathbb{R}} \widehat{\phi} = 1$, and $\widehat{\phi}$ decays exponentially away from zero. Then we can define the test function $\mathbf{m}(x) = (0, \phi(x), sign(x)\sqrt{1-\phi^2(x)})$, where ϕ is the inverse Fourier transform of the function $\widehat{\phi}$. Consider now $\mathbf{m}_\delta(x) = \mathbf{m}(\frac{x}{\delta^{1/3}})$. The conditions on the function ϕ ensure that $\mathbf{m}$ belongs to the set $\mathscr{A}_b$ defined earlier. The exchange energy can be easily computed:

$$E_{ex} = \frac{1}{2}\frac{1}{\delta^{1/3}}\int_{\mathbb{R}} |\mathbf{m}'|^2\, dx. \tag{7.9}$$

The self-induced energy can be easily estimated too:

$$E_M = \frac{1}{2}\int_{\mathbb{R}} \widehat{m}^2_{\delta,2}(\xi)\widehat{\Gamma}_\delta(\xi)\, d\xi = \frac{1}{\delta^{1/3}}\int_0^\infty \widehat{\phi}^2(\xi)\frac{1-e^{-\delta^{2/3}\xi}}{\xi}\, d\xi. \tag{7.10}$$

Now, since ϕ is smooth and $\phi(0) = 0$, by Watson's lemma, we obtain:

$$E_M \sim \frac{1}{\delta^{1/3}}\int_0^\infty \frac{\widehat{\phi}^2(\xi)}{\xi}\, d\xi + \sum_{n=1}^{\infty}\frac{a_n n!}{\delta^{(2n+1)/3}}, \tag{7.11}$$

where $\frac{\widehat{\phi}^2(\xi)}{\xi} \sim \sum_{n=1}^\infty a_n\xi^n$ in a neighbourhood of zero.

We summarize these results in the following.

Theorem 7.1 *Consider the Bloch wall functional without anisotropy*

$$F^b_{0,\delta}[\mathbf{m}] = \frac{1}{2}\int_{\mathbb{R}} |\mathbf{m}'|^2 + \frac{1}{2}\int_{\mathbb{R}} m_2\,(\Gamma_\delta * m_2)$$

and $\mathscr{A}_b = \{\mathbf{m}\in\mathscr{A}|\ m_1 = 0\}$. *There exist (nonnegative) constants* c_0 *and* C_0 *such that*

$$c_0\delta^{-1/3} \leqslant \min_{\mathbf{m}\in\mathscr{A}_b} F^b_{0,\delta}[\mathbf{m}] \leqslant C_0\delta^{-1/3}. \tag{7.12}$$

7.3 Asymptotic analysis for the Bloch Wall

Define $m_2 = g$, $m_1 = 0$, and $m_3 = \text{sign}(x)\sqrt{1-g^2}$. We consider the functional

$$F_\delta[g] = \frac{1}{2}\int_{\mathbb{R}} (g')^2 + \int_{\mathbb{R}} (g * \Gamma_\delta)\, g \tag{7.13}$$

Downloaded from https://www.cambridge.org/core. Lehrst F Alte Geschichte Hist Inst, on 06 Jun 2017 at 07:46:52, subject to the Cambridge Core terms of use, available at https://www.cambridge.org/core/terms. https://doi.org/10.1017/S0956792504005595

and the variational problem:

$$\min_{g(0)=1} F_\delta[g]. \tag{7.14}$$

As before, we find an expression for the solution in terms of its Fourier transform:

$$g(x) = C \int_0^\infty \frac{\cos(\xi x)}{\xi^2 + \widehat{\Gamma}_\delta(\xi)}\, d\xi, \tag{7.15}$$

where C is such that $g(0) = 1$:

$$C = \frac{1}{\int_0^\infty \frac{1}{\xi^2 + \widehat{\Gamma}_\delta(\xi)}\, d\xi}. \tag{7.16}$$

We are going to derive an asymptotic expression for the function g as $\delta \to \infty$. To do that, we split the interval of integration into two, and drop the constant C for clarity of notation. We will renormalize the function in the end. In each subinterval of integration, we substitute the function $\widehat{\Gamma}_\delta$ by an approximation:

$$g(x) = \int_0^{\frac{1}{\delta}} \frac{\cos(\xi x)}{\xi^2 + 1 - \delta\xi + \frac{\delta^2}{2}\xi^2}\, d\xi + \int_{\frac{1}{\delta}}^\infty \frac{\cos(\xi x)}{\xi^2 + \frac{1}{\delta\xi}}\, d\xi \tag{7.17}$$

Now we deal with the two integrals separately. The first integral can be written as:

$$\begin{aligned} I_1(x) &= \int_0^{\frac{1}{\delta}} \frac{\cos(\xi x)}{\xi^2 + 1 - \delta\xi + \frac{\delta^2}{2}\xi^2}\, d\xi \\ &= \int_0^{\frac{1}{\delta}} \frac{\cos(\xi x)}{\left(\sqrt{1+\frac{\delta^2}{2}}\xi - \frac{\delta}{2\sqrt{1+\frac{\delta^2}{2}}}\right)^2 + 1 - \frac{\delta^2}{4\left(1+\frac{\delta^2}{2}\right)}}\, d\xi. \end{aligned}$$

The expression for the coefficients are too complicated, so we approximate them for clarity of notation:

$$\sqrt{1+\frac{\delta^2}{2}} \sim \frac{\delta}{\sqrt{2}} \quad \text{as } \delta \to \infty \tag{7.18}$$

$$\frac{\delta}{2\sqrt{1+\frac{\delta^2}{2}}} \sim \frac{1}{\sqrt{2}} \quad \text{as } \delta \to \infty \tag{7.19}$$

$$1 - \frac{\delta^2}{4\left(1+\frac{\delta^2}{2}\right)} \sim \frac{1}{2} \quad \text{as } \delta \to \infty. \tag{7.20}$$

Now we can rewrite the expression for I_1 as

$$\begin{aligned} I_1(x) &= \int_0^{\frac{1}{\delta}} \frac{\cos(\xi x)}{\left(\frac{\delta}{\sqrt{2}}\xi - \frac{1}{\sqrt{2}}\right)^2 + \frac{1}{2}}\, d\xi = \frac{\sqrt{2}}{\delta} \int_{-1}^0 \frac{\cos(\frac{t+1}{\delta}x)}{1+t^2}\, dt \\ &= \frac{\sqrt{2}}{\delta}\cos\left(\frac{x}{\delta}\right) \int_0^1 \frac{\cos(t\frac{x}{\delta})}{1+t^2}\, dt + \frac{\sqrt{2}}{\delta}\sin\left(\frac{x}{\delta}\right) \int_0^1 \frac{\sin(t\frac{x}{\delta})}{1+t^2}\, dt. \end{aligned} \tag{7.21}$$

Downloaded from https://www.cambridge.org/core. Lehrst F Alte Geschichte Hist Inst, on 06 Jun 2017 at 07:46:52, subject to the Cambridge Core terms of use, available at https://www.cambridge.org/core/terms. https://doi.org/10.1017/S0956792504005595

Now we can write a representation of the function in two regimes:

$$I_1(x) \sim \frac{\sqrt{2}}{\delta}\frac{\pi}{4} - \frac{\sqrt{2}}{\delta}\left(1 - \frac{\log 2}{2}\right)\frac{x^2}{\delta^2} \quad \text{if } \left|\frac{x}{\delta}\right| \ll 1 \tag{7.22}$$

$$I_1(x) \sim \frac{\sqrt{2}}{\delta}\frac{\delta}{x}\sin\left(\frac{x}{\delta}\right) - \frac{\sqrt{2}}{2\delta}\frac{\delta^2}{x^2} \quad \text{if } \left|\frac{x}{\delta}\right| \gg 1. \tag{7.23}$$

We turn now to the expression for I_2:

$$I_2(x) = \int_{\frac{1}{\delta}}^{\infty} \frac{\xi\cos(\xi x)}{\xi^3 + \frac{1}{\delta}}\,d\xi = \delta^{\frac{1}{3}}\int_{\delta^{-\frac{2}{3}}}^{\infty} \frac{t\cos\left(t\frac{x}{\delta^{\frac{1}{3}}}\right)}{t^3+1}\,dt. \tag{7.24}$$

To obtain an expression for I_2 when $|\frac{x}{\delta}| \ll 1$, we express the integral in the following form, using residues:

$$\begin{aligned} I_2(x) = {} & \delta^{\frac{1}{3}}\frac{\pi}{\sqrt{3}}\left(\cos\left(\frac{x}{2\delta^{\frac{1}{3}}}\right) - \frac{\sqrt{3}}{3}\sin\left(\frac{x}{2\delta^{\frac{1}{3}}}\right)\right)e^{-\frac{\sqrt{3}x}{2\delta^{\frac{1}{3}}}} - \delta^{\frac{1}{3}}\int_0^{\infty}\frac{te^{-\frac{tx}{\delta^{\frac{1}{3}}}}}{t^6+1}\,dt \\ & - \delta^{\frac{1}{3}}\int_0^{\delta^{-\frac{2}{3}}}\frac{t\cos\left(t\frac{x}{\delta^{\frac{1}{3}}}\right)}{t^3+1}\,dt. \end{aligned} \tag{7.25}$$

Now we can derive the behaviour of the function for $|\frac{x}{\delta^{\frac{1}{3}}}| \ll 1$. We will make use of the following:

$$\int_0^{\infty}\frac{t}{t^6+1}\,dt = \frac{\pi\sqrt{3}}{9}$$

$$\int_0^{\infty}\frac{t^2}{t^6+1}\,dt = \frac{\pi}{6}$$

$$\int_0^{\delta^{-\frac{2}{3}}}\frac{t}{t^3+1}\,dt \sim \frac{1}{2\delta^{\frac{4}{3}}} + O\left(\delta^{-\frac{10}{3}}\right).$$

With this, we obtain

$$I_2(x) \sim \delta^{\frac{1}{3}}\pi\left(\left(1 - \frac{\sqrt{3}}{9} - \frac{1}{2\pi}\delta^{-\frac{4}{3}}\right) - \frac{1}{4}\frac{x}{\delta^{\frac{1}{3}}} + O\left(\frac{x^2}{\delta^2}\right)\right) \quad \text{if } |x| \ll \delta^{\frac{1}{3}},$$

$$I_2(x) \sim -\delta^{\frac{1}{3}}\left(\frac{\delta^{\frac{2}{3}}}{x^2} - 3\frac{\delta^{-\frac{4}{3}}}{x^2}\right) \quad \text{if } \delta^{\frac{1}{3}} \ll |x| \ll \delta,$$

$$I_2(x) \sim -\delta^{\frac{1}{3}}\left(-\frac{\delta^{-\frac{1}{3}}}{x}\sin\left(\frac{x}{\delta}\right) + \frac{\delta^{\frac{2}{3}}}{x^2}\cos\left(\frac{x}{\delta}\right)\right) \quad \text{if } |x| \gg \delta. \tag{7.26}$$

When we combine I_1 and I_2 we obtain

$$I_1 + I_2 \sim \frac{\sqrt{2}}{\delta}\frac{\pi}{4} + \delta^{\frac{1}{3}}\pi\left(\left(1 - \frac{\sqrt{3}}{9} - \frac{1}{2\pi}\delta^{-\frac{4}{3}}\right) - \frac{1}{4}\frac{x}{\delta^{\frac{1}{3}}} + O\left(\frac{x^2}{\delta^2}\right)\right) \quad \text{if } |x| \ll \delta^{\frac{1}{3}},$$

$$I_1 + I_2 \sim \frac{\sqrt{2}}{\delta}\frac{\pi}{4} - \frac{\sqrt{2}}{\delta}\left(1 - \frac{\log 2}{2}\right)\frac{x^2}{\delta^2} - \delta^{\frac{1}{3}}\left(\frac{\delta^{\frac{2}{3}}}{x^2} - 3\frac{\delta^{-\frac{4}{3}}}{x^2}\right) \quad \text{if } \delta^{\frac{1}{3}} \ll |x| \ll \delta,$$

$$I_1 + I_2 \sim \frac{\sqrt{2}}{\delta}\frac{\delta}{x}\sin\left(\frac{x}{\delta}\right) - \frac{\sqrt{2}}{2\delta}\frac{\delta^2}{x^2} - \frac{\sin\left(\frac{x}{\delta}\right)}{x} + \frac{\delta\cos\left(\frac{x}{\delta}\right)}{x^2} \quad \text{if } |x| \gg \delta.$$

Downloaded from https://www.cambridge.org/core. Lehrst F Alte Geschichte Hist Inst, on 06 Jun 2017 at 07:46:52, subject to the Cambridge Core terms of use, available at https://www.cambridge.org/core/terms. https://doi.org/10.1017/S0956792504005595

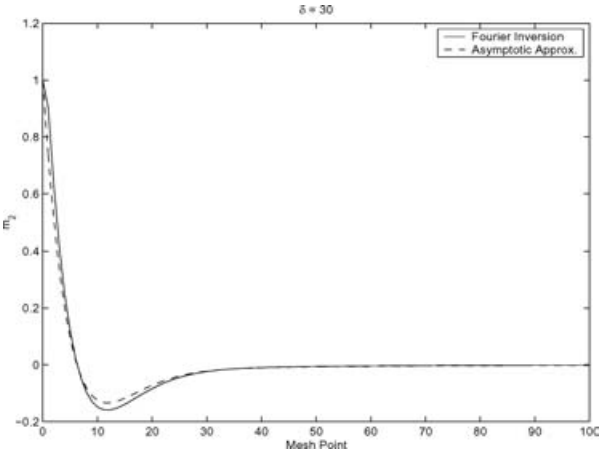

FIGURE 11. Fourier inversion vs. Asymptotic approximation.

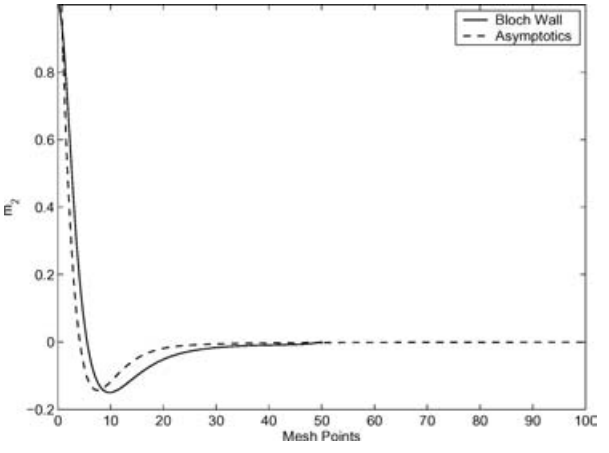

FIGURE 12. Comparison of the Bloch wall profile obtained with our energy minimization algorithm and the approximation obtained via Fourier transform. The parameters used are $L = 100$, $\delta = 10$, and $q = 0.045$.

Now we need to rescale by $I_1(0) + I_2(0)$. Doing this, we obtain that the constant C we had before is of order $C = O(\delta^{-\frac{1}{3}})$. Keeping the leading order in δ, the solution is

$$g(x) \sim 1 - \frac{1}{1 - \frac{\sqrt{3}}{9}} \frac{x}{\delta^{\frac{1}{3}}} + O\left(\frac{x^2}{\delta^2}\right) \quad \text{if } |x| \ll \delta^{\frac{1}{3}},$$

$$g(x) \sim -\frac{1}{\pi\left(1 - \frac{\sqrt{3}}{9}\right)} \frac{\delta^{\frac{2}{3}}}{x^2} \cos\left(\frac{x}{\delta}\right) \quad \text{if } |x| \gg \delta^{\frac{1}{3}}. \tag{7.27}$$

As we did in the case of the Néel wall, we obtain that the energy is precisely $\frac{C}{2} \sim c_o \delta^{-\frac{1}{3}}$, consistent with the lower bound obtained previously.

Downloaded from https://www.cambridge.org/core. Lehrst F Alte Geschichte Hist Inst, on 06 Jun 2017 at 07:46:52, subject to the Cambridge Core terms of use, available at https://www.cambridge.org/core/terms. https://doi.org/10.1017/S0956792504005595

We have computed the solution by numerical inversion of the Fourier Transform and compared the result with the function I_2 for a few values of δ. The Fourier Transform was computed using a Hurwitz–Zweifel expansion, combined with a Clenshaw–Curtis quadrature [22]. In Figure 11 we show the results for $\delta = 30$. As we can see, the function I_2 captures both the core length and the amplitude of the oscillations. In figure 12 we compare the Bloch wall obtained with our energy minimization algorithm and the inverse Fourier transform (7.17) for $L = 100$, $\delta = 10.$, and $q = 0.045$. As in the Néel wall case, we manage to capture the relevant length scales and the main features in the profile, even though the details in the core might not be accurate.

8 Concluding remarks

A new model for the study of thin films has been derived from the Landau–Lifshitz energy functional. The one-dimensional model studied in this article has been derived from this thin film model. Using this model we have analyzed the structure of one-dimensional magnetic domain walls in uniaxial ferromagnetic materials, and in particular, the structure of the Néel and Bloch walls. The main findings are the following:

- There exists a critical thickness δ_c at which the energy of the Néel wall is equal to the energy of the Bloch wall. For $\delta < \delta_c$, the Néel wall is energetically favourable, while for $\delta > \delta_c$, the Bloch wall is preferred.
- The Néel wall possesses a long, logarithmic tail. For a fixed value $\delta > 0$, we have obtained the optimal energy scaling (1.8). The compactness of the minimizing sequences is of the one-dimensional functional is lost as $q \to 0$.
- The Bloch wall is localized, and the decay is algebraic. For $q = 0$, minimizing sequences of the Bloch wall energy functional are precompact, and we have obtained the optimal energy scaling (1.9).

We have implemented a modified Newton's method for energy minimization and illustrated all our findings numerically.

Acknowledgements

I would like to thank my thesis advisor, Prof. Weinan E, for his guidance, and for suggesting this problem to me. I am also grateful to Prof. Robert V. Kohn, and Prof. Stefan Müller for helpful discussions.

9 Appendix A: The thin film model

It has been observed experimentally that in a thin film the magnetization does not depend on the thickness variable. This has been understood in the sense of Γ-convergence in

Downloaded from https://www.cambridge.org/core. Lehrst F Alte Geschichte Hist Inst, on 06 Jun 2017 at 07:46:52, subject to the Cambridge Core terms of use, available at https://www.cambridge.org/core/terms. https://doi.org/10.1017/S0956792504005595

Gioia & James [16]. In this appendix we derive a reduced model for thin films by assuming that the magnetization is independent of the thickness variable. The model presented was derived in García-Cervera [13] and has been used for the analysis and simulations of the Landau–Lifshitz equations elsewhere [23, 15, 14, 10, 11].

Assume that $\mathbf{m}(x, y, z) = \mathbf{m}(x, y)$ for $(x, y, z) \in \Omega \times [-\delta, \delta] \subset \mathbb{R}^3$. We denote $\mathbf{x} = (x, y)$, and $\mathbf{x}' = (x, y, z) = (\mathbf{x}, z)$. The anisotropy and exchange terms in the Landau–Lifshitz functional (1.1) become

$$\begin{aligned} E_a &= \delta q \int_\Omega \Phi(\mathbf{m})\, d\mathbf{x}, \\ E_{ex} &= \delta \int_\Omega |\nabla \mathbf{m}|^2\, d\mathbf{x}. \end{aligned} \tag{9.1}$$

We consider now the stray field energy. Recall that the stray field is $\mathbf{h}_s = -\nabla u$, where u satisfies

$$\begin{aligned} \Delta u &= \nabla \cdot \mathbf{m} \quad \text{in } V, \\ \Delta u &= 0 \quad \text{in } \overline{V}^c, \\ [u]_{|\partial V} &= 0, \\ \left[\frac{\partial u}{\partial v}\right]_{|\partial V} &= -\mathbf{m} \cdot v. \end{aligned} \tag{9.2}$$

The solution to this equation is given by

$$\begin{aligned} u(\mathbf{x}') &= \int_V \nabla N(\mathbf{x}' - \mathbf{y}') \cdot \mathbf{m}(\mathbf{y})\, d\mathbf{y}' = \nabla N * \mathbf{m} \\ &= \int_V N(\mathbf{x}' - \mathbf{y}')\, \nabla \cdot \mathbf{m}(\mathbf{y}')\, d\mathbf{y}' - \int_{\partial V} N(\mathbf{x}' - \mathbf{z}')\, \mathbf{m} \cdot v(\mathbf{z}')\, d\sigma(\mathbf{z}'), \end{aligned} \tag{9.3}$$

where $N(\mathbf{x}') = -\frac{1}{4\pi|\mathbf{x}'|}$ is the Newtonian potential in $\mathbb{R}^3$.

Since $\mathbf{m}$ is only a function of (x, y), we can integrate with respect to the z variable in the expression for u. The stray field energy can be written as:

$$2E_M = \int_V \nabla u(\mathbf{x}') \cdot \mathbf{m}(\mathbf{x}')\, d\mathbf{x} = -\int_V u(\mathbf{x}') \nabla \cdot\ \mathbf{m}(\mathbf{x}')\, d\mathbf{x}' + \int_{\partial V} u(\mathbf{x}')(\mathbf{m} \cdot v)(\mathbf{x}')\, d\sigma(\mathbf{x}'). \tag{9.4}$$

For notational convenience we denote $\nabla \cdot \mathbf{m} = \rho$. Substituting in the expression for E_M the expression for u:

$$\begin{aligned} 2E_M = &-\int_V \int_V \rho(\mathbf{x}') N(\mathbf{x}' - \mathbf{y}') \rho(\mathbf{y}')\, d\mathbf{x}' d\mathbf{y}' + 2 \int_{\partial V} \int_V \rho(\mathbf{x}') N(\mathbf{x}' - \mathbf{y}')(\mathbf{m} \cdot v)(\mathbf{y}')\, d\mathbf{x}'\, d\sigma(\mathbf{y}') \\ &- \int_{\partial V} \int_{\partial V} (\mathbf{m} \cdot v)(\mathbf{x}') N(\mathbf{x}' - \mathbf{y}')(\mathbf{m} \cdot v)(\mathbf{y}')\, d\sigma(\mathbf{x}')\, d\sigma(\mathbf{y}'). \end{aligned} \tag{9.5}$$

Downloaded from https://www.cambridge.org/core. Lehrst F Alte Geschichte Hist Inst, on 06 Jun 2017 at 07:46:52, subject to the Cambridge Core terms of use, available at https://www.cambridge.org/core/terms. https://doi.org/10.1017/S0956792504005595

Now we rewrite the energy, integrating with respect to z. The bulk energy term becomes:

$$-\int_V\int_V \rho(\mathbf{x}')N(\mathbf{x}'-\mathbf{y}')\rho(\mathbf{y}')\,d\mathbf{x}'\,d\mathbf{y}' = -\int_\Omega\int_\Omega \rho(\mathbf{x})\left(\int_{-\delta}^{\delta}\int_{-\delta}^{\delta} N(\mathbf{x}-\mathbf{y},z-p)\,dpdz\right)\rho(\mathbf{y})\,d\mathbf{x}\,d\mathbf{y}. \tag{9.6}$$

We need to integrate the Newtonian Potential. To simplify the notation, we define $R=\sqrt{(x-s)^2+(y-t)^2}$. Now we integrate:

$$\int_{-\delta}^{\delta}\frac{1}{\sqrt{R^2+(z-p)^2}}\,dp = \sinh^{-1}\left(\frac{z+\delta}{R}\right)-\sinh^{-1}\left(\frac{z-\delta}{R}\right), \tag{9.7}$$

where $\sinh^{-1}(x)=\log(x+\sqrt{1+x^2})$ is the inverse of the hyperbolic sine. Define

$$\Theta_\delta(x,y,z)=\frac{1}{4\pi}\sinh^{-1}\left(\frac{z+\delta}{\sqrt{x^2+y^2}}\right)-\frac{1}{4\pi}\sinh^{-1}\left(\frac{z-\delta}{\sqrt{x^2+y^2}}\right). \tag{9.8}$$

We integrate again to obtain an expression for the energy

$$\int_{-\delta}^{\delta}\int_{-\delta}^{\delta}\frac{1}{\sqrt{R^2+(z-p)^2}}\,dpdz = 4\delta\sinh^{-1}\left(\frac{2\delta}{R}\right)-2(\sqrt{R^2+4\delta^2}-R). \tag{9.9}$$

In view of this, we define a new potential:

$$\widetilde{K}_\delta(\mathbf{x})=\frac{\delta}{\pi}\sinh^{-1}\left(\frac{2\delta}{|\mathbf{x}|}\right)-\frac{1}{2\pi}(\sqrt{|\mathbf{x}|^2+4\delta^2}-|\mathbf{x}|)\quad \mathbf{x}\in\mathbb{R}^2\backslash\{(0,0)\}. \tag{9.10}$$

The bulk energy becomes

$$-\int_V\int_V \rho(\mathbf{x}')N(\mathbf{x}'-\mathbf{y}')\rho(\mathbf{y}')\,d\mathbf{x}'d\mathbf{y}' = \int_\Omega\int_\Omega \rho(\mathbf{x})\widetilde{K}_\delta(\mathbf{x}-\mathbf{y})\rho(\mathbf{y})\,d\mathbf{x}\,d\mathbf{y}. \tag{9.11}$$

Now we rewrite the terms that involve boundary integrals. Note that $\partial V=\partial\Omega\times[-\delta,\delta]\cup\Omega\times\{\delta\}\cup\Omega\times\{-\delta\}$. With this in mind:

$$\begin{aligned}
&\int_{\partial V}\int_V \rho(\mathbf{x}')N(\mathbf{x}'-\mathbf{y}')(\mathbf{m}\cdot\nu)(\mathbf{y}')\,d\mathbf{x}'\,d\sigma(\mathbf{y}')\\
&\quad=-\int_\Omega\int_{\partial\Omega}\rho(\mathbf{x})\widetilde{K}_\delta(\mathbf{x}-\mathbf{y})(\mathbf{m}\cdot\nu)(\mathbf{y})\,d\mathbf{x}\,d\sigma(\mathbf{y})\\
&\qquad-\int_\Omega\int_\Omega\rho(\mathbf{x})(\Theta_\delta(\mathbf{x}-\mathbf{y},\delta)-\Theta_\delta(\mathbf{x}-\mathbf{y},-\delta))m_3(\mathbf{y})\,d\mathbf{x}\,d\mathbf{y}\\
&\quad=-\int_\Omega\int_{\partial\Omega}\rho(\mathbf{x})\widetilde{K}_\delta(\mathbf{x}-\mathbf{y})(\mathbf{m}\cdot\nu)(\mathbf{y})\,d\mathbf{x}\,d\sigma(\mathbf{y}).
\end{aligned} \tag{9.12}$$

this last equality because $\Theta_\delta(x,y,z)=\Theta_\delta(x,y,-z)$. Finally, the last term becomes:

Downloaded from https://www.cambridge.org/core. Lehrst F Alte Geschichte Hist Inst, on 06 Jun 2017 at 07:46:52, subject to the Cambridge Core terms of use, available at https://www.cambridge.org/core/terms. https://doi.org/10.1017/S0956792504005595

$$\begin{aligned}
&\int_{\partial V}\int_{\partial V}(\mathbf{m}\cdot\nu)(\mathbf{x}')N(\mathbf{x}'-\mathbf{y}')(\mathbf{m}\cdot\nu)(\mathbf{y}')\,d\sigma(\mathbf{x}')\,d\sigma(\mathbf{y}')\\
&\quad=-\int_{\partial\Omega}\int_{\partial\Omega}(\mathbf{m}\cdot\nu)(\mathbf{x})\widetilde{K}_\delta(\mathbf{x}-\mathbf{y})(\mathbf{m}\cdot\nu(\mathbf{y}))\,d\sigma(\mathbf{x})\,d\sigma(\mathbf{y})\\
&\qquad-\int_{\Omega}\int_{\partial\Omega}m_3(\mathbf{x})\Theta_\delta(\mathbf{x}-\mathbf{y},\delta)(\mathbf{m}\cdot\nu)(\mathbf{y})\,d\sigma(\mathbf{y})\,d\mathbf{x}\\
&\qquad+\int_{\Omega}\int_{\partial\Omega}m_3(\mathbf{x})\Theta_\delta(\mathbf{x}-\mathbf{y},-\delta)(\mathbf{m}\cdot\nu)(\mathbf{y})\,d\sigma(\mathbf{y})\,d\mathbf{x}\\
&\qquad-\int_{\partial\Omega}\int_{\Omega}(\mathbf{m}\cdot\nu)(\mathbf{x})\Theta_\delta(\mathbf{x}-\mathbf{y},\delta)m_3(\mathbf{y})\,d\mathbf{y}d\sigma(\mathbf{x})+\int_{\Omega}\int_{\Omega}m_3(\mathbf{x})N(\mathbf{x}-\mathbf{y},0)m_3(\mathbf{y})\,d\mathbf{x}\,d\mathbf{y}\\
&\qquad-\int_{\Omega}\int_{\Omega}m_3(\mathbf{x})N(\mathbf{x}-\mathbf{y},2\delta)m_3(\mathbf{y})\,d\mathbf{x}\,d\mathbf{y}+\int_{\partial\Omega}\int_{\Omega}(\mathbf{m}\cdot\nu)(\mathbf{x})\Theta_\delta(\mathbf{x}-\mathbf{y},\delta)m_3(\mathbf{y})\,d\mathbf{y}\,d\sigma(\mathbf{x})\\
&\qquad-\int_{\Omega}\int_{\Omega}m_3(\mathbf{x})N(\mathbf{x}-\mathbf{y},2\delta)m_3(\mathbf{y})\,d\mathbf{x}\,d\mathbf{y}+\int_{\Omega}\int_{\Omega}m_3(\mathbf{x})N(\mathbf{x}-\mathbf{y},0)m_3(\mathbf{y})\,d\mathbf{x}\,d\mathbf{y}. \qquad (9.13)
\end{aligned}$$

Simplifying this last expression, we obtain:

$$\begin{aligned}
&\int_{\partial V}\int_{\partial V}(\mathbf{m}\cdot\nu)(\mathbf{x}')N(\mathbf{x}'-\mathbf{y}')(\mathbf{m}\cdot\nu)(\mathbf{y}')\,d\sigma(\mathbf{x}')\,d\sigma(\mathbf{y}')\\
&\quad=-\int_{\partial\Omega}\int_{\partial\Omega}(\mathbf{m}\cdot\nu)(\mathbf{x})\widetilde{K}_\delta(\mathbf{x}-\mathbf{y})(\mathbf{m}\cdot\nu)(\mathbf{y})\,d\sigma(\mathbf{x})\,d\sigma(\mathbf{y})\\
&\qquad+2\int_{\Omega}\int_{\Omega}m_3(\mathbf{x})\left(N(\mathbf{x}-\mathbf{y},0)-N(\mathbf{x}-\mathbf{y},2\delta)\right)m_3(\mathbf{y})\,d\mathbf{x}\,d\mathbf{y}. \qquad (9.14)
\end{aligned}$$

To obtain the effective stray field energy, we rescale by the thickness. We define two new kernels:

$$\begin{aligned}
K_\delta(\mathbf{x})&=\frac{1}{2\delta}\widetilde{K}_\delta(\mathbf{x})=\frac{1}{2\pi}\sinh^{-1}\left(\frac{2\delta}{|\mathbf{x}|}\right)-\frac{1}{4\pi\delta}\left(\sqrt{|\mathbf{x}|^2+4\delta^2}-|\mathbf{x}|\right)\\
W_\delta(\mathbf{x})&=-\frac{N(\mathbf{x}-\mathbf{y},0)-N(\mathbf{x}-\mathbf{y},2\delta)}{\delta}=\frac{1}{4\pi\delta}\left(\frac{1}{|\mathbf{x}|}-\frac{1}{\sqrt{|\mathbf{x}|^2+4\delta^2}}\right).
\end{aligned} \qquad (9.15)$$

Then, we can write the self-induced energy as:

$$\begin{aligned}
2E_M=&\int_{\Omega}\int_{\Omega}\rho(\mathbf{x})K_\delta(\mathbf{x}-\mathbf{y})\rho(\mathbf{y})\,d\mathbf{x}\,d\mathbf{y}-2\int_{\Omega}\int_{\partial\Omega}\rho(\mathbf{x})K_\delta(\mathbf{x}-\mathbf{y})(\mathbf{m}\cdot\nu)(\mathbf{y})\,d\mathbf{x}\,d\sigma(\mathbf{y})\\
&+\int_{\partial\Omega}\int_{\partial\Omega}(\mathbf{m}\cdot\nu)(\mathbf{x})K_\delta(\mathbf{x}-\mathbf{y})(\mathbf{m}\cdot\nu)(\mathbf{y})\,d\sigma(\mathbf{x})\,d\sigma(\mathbf{y})\\
&+\int_{\Omega}\int_{\Omega}m_3(\mathbf{x})W_\delta(\mathbf{x}-\mathbf{y})m_3(\mathbf{y})\,d\mathbf{x}\,d\mathbf{y}. \qquad (9.16)
\end{aligned}$$

We denote by $\mathbf{m}'=(m_1,m_2)$ the *in plane* components of the magnetization. After integration by parts, we can write the energy as

$$E_M=\frac{1}{2}\int_{\Omega}\mathbf{m}'\nabla(\nabla K_\delta * \mathbf{m}')\,d\mathbf{x}+\frac{1}{2}\int_{\Omega}m_3\,(W_\delta * m_3)\,d\mathbf{x}.$$

Downloaded from https://www.cambridge.org/core. Lehrst F Alte Geschichte Hist Inst, on 06 Jun 2017 at 07:46:52, subject to the Cambridge Core terms of use, available at https://www.cambridge.org/core/terms. https://doi.org/10.1017/S0956792504005595

10 Appendix B: Fourier space representation of the thin film model

Using Plancherel's theorem, we can write the stray field energy in the following way:

$$E_M = \frac{1}{2}\int_V \nabla u \cdot \mathbf{m}\, d\mathbf{x} = \frac{1}{2}\int_{\mathbb{R}^3} \widehat{\nabla u}(\widehat{\mathbf{m}\chi_V})\, d\xi = \frac{1}{2}\int_{\mathbb{R}^3} (\xi\widehat{u}) \cdot (\widehat{\mathbf{m}\chi_V})\, d\xi.$$

We know that $u = \nabla N * \mathbf{m}$, and N is the Newtonian Potential, so the Fourier transform of the magnetostatic potential is

$$\widehat{u}(\xi) = (\xi\widehat{N}) \cdot \widehat{\mathbf{m}} = \frac{1}{|\xi|^2}(\xi \cdot \widehat{\mathbf{m}}).$$

Putting it all together, we obtain the expression

$$E_M = \frac{1}{2}\int_{\mathbb{R}^3} \frac{(\xi \cdot (\widehat{\mathbf{m}\chi_V}))^2}{|\xi|^2}\, d\xi.$$

We introduce the following notation: $\xi = (\xi', \xi_3)$, $x = (\mathbf{x}', z)$, and $\mathbf{m} = (\mathbf{m}', m_3)$. The Fourier Transform of $\mathbf{m}\chi_V$ is:

$$\begin{aligned}(\widehat{\mathbf{m}\chi_V})(\xi) &= \int_V e^{-2\pi i\xi\cdot x}\mathbf{m}(x)\, dx = \int_\Omega e^{-2\pi i\xi'\cdot\mathbf{x}'}\int_{-\delta}^{\delta} e^{-2\pi i\xi_3 z}\, dz\, d\mathbf{x}' \\ &= (\widehat{\mathbf{m}\chi_\Omega})\frac{\sin 2\pi\delta\xi_3}{\pi\xi_3}. \end{aligned} \tag{10.1}$$

Hence the induced field can be written as

$$\begin{aligned} 2E_M &= \int_{\mathbb{R}^3} \frac{(\xi'\cdot\widehat{\mathbf{m}}' + \xi_3\widehat{\mathbf{m}}_3)^2}{|\xi|^2}\, d\xi = \int_{\mathbb{R}^3} \frac{(\xi'\cdot\widehat{\mathbf{m}}')^2 + 2(\xi_3\widehat{\mathbf{m}}_3)(\xi'\cdot\widehat{\mathbf{m}}') + (\xi_3\widehat{\mathbf{m}}_3)^2}{|\xi|^2}\, d\xi \\ &= \int_{\mathbb{R}^2} (\xi'\cdot\widehat{\mathbf{m}}')^2 \int_{\mathbb{R}} \frac{\sin^2(2\pi\delta\xi_3)}{\pi^2\xi_3^2}\frac{1}{|\xi'|^2+\xi_3^2}\, d\xi_3\, d\xi' \\ &\quad + 2\int_{\mathbb{R}^2} (\xi'\cdot\widehat{\mathbf{m}}')\widehat{\mathbf{m}}_3 \int_{\mathbb{R}} \frac{\sin^2(2\pi\delta\xi_3)}{\pi^2\xi_3^2}\frac{\xi_3}{|\xi'|^2+\xi_3^2}\, d\xi_3\, d\xi' \\ &\quad + \int_{\mathbb{R}^2} \widehat{\mathbf{m}}_3^2 \int_{\mathbb{R}} \frac{\sin^2(2\pi\delta\xi_3)}{\pi^2\xi_3^2}\frac{\xi_3^2}{|\xi'|^2+\xi_3^2}\, d\xi_3\, d\xi'. \end{aligned} \tag{10.2}$$

Observe that the middle integral vanishes, since the integrand is an odd function of ξ_3. Finally, we obtain the expression for the Magnetostatic Energy in Fourier Space:

$$\begin{aligned} 2E_M &= \int_{\mathbb{R}^2} (\xi'\cdot\widehat{\mathbf{m}}')^2 \int_{\mathbb{R}} \frac{\sin^2(2\pi\delta\xi_3)}{\pi^2\xi_3^2}\frac{1}{|\xi'|^2+\xi_3^2}\, d\xi_3\, d\xi' \\ &\quad + \int_{\mathbb{R}^2} \widehat{\mathbf{m}}_3^2 \int_{\mathbb{R}} \frac{\sin^2(2\pi\delta\xi_3)}{\pi^2}\frac{1}{|\xi'|^2+\xi_3^2}\, d\xi_3\, d\xi'. \end{aligned} \tag{10.3}$$

Downloaded from https://www.cambridge.org/core. Lehrst F Alte Geschichte Hist Inst, on 06 Jun 2017 at 07:46:52, subject to the Cambridge Core terms of use, available at https://www.cambridge.org/core/terms. https://doi.org/10.1017/S0956792504005595

Comparing this expression with the expression we had obtained before, we observe that

$$\widehat{K}_\delta(\xi) = \frac{1}{2\delta}\int_{\mathbb{R}} \frac{\sin^2(2\pi\delta\xi_3)}{\pi^2\xi_3^2}\frac{1}{|\xi'|^2+\xi_3^2}\,d\xi_3 \tag{10.4}$$

$$\widehat{W}_\delta(\xi) = \frac{1}{2\delta}\int_{\mathbb{R}} \frac{\sin^2(2\pi\delta\xi_3)}{\pi^2}\frac{1}{|\xi'|^2+\xi_3^2}\,d\xi_3. \tag{10.5}$$

or, making the change of variables $\eta = \delta\xi_3$,

$$\widehat{K}_\delta(\xi) = \frac{\delta^2}{2\pi^2}\int_{\mathbb{R}} \frac{\sin^2(2\pi\eta)}{\eta^2}\frac{1}{\delta^2|\xi'|^2+\eta^2}\,d\eta \tag{10.6}$$

$$\widehat{W}_\delta(\xi) = \frac{\delta}{\pi^2}\int_{\mathbb{R}} \frac{\sin^2(2\pi\eta)}{\delta^2|\xi'|^2+\eta^2}\,d\eta. \tag{10.7}$$

Both integrals can be easily computed using the theory of residues, and after we do this, we obtain:

$$\widehat{K}_\delta(\xi) = \frac{1}{|\xi|^2}(1-\widehat{\Gamma}_\delta(|\xi|)) \tag{10.8}$$

$$\widehat{W}_\delta(\xi) = \widehat{\Gamma}_\delta(|\xi|), \tag{10.9}$$

where

$$\widehat{\Gamma}_\delta(t) = \frac{1-e^{-4\pi\delta|t|}}{4\pi\delta|t|} \quad t\in\mathbb{R}. \tag{10.10}$$

The self-induced energy can be written in Fourier space as

$$E_M = \frac{1}{2}\int_{\mathbb{R}^2}\frac{(\xi\cdot\mathbf{m}')^2}{|\xi|^2}(1-\widehat{\Gamma}_\delta(|\xi|))\,d\xi + \frac{1}{2}\int_{\mathbb{R}^2}\widehat{m}_3^2\widehat{\Gamma}_\delta(|\xi|)\,d\xi.$$

Note that as $\delta\to 0$ the self-induced energy becomes

$$E_M = \frac{1}{2}\int_V m_3^2\,d\mathbf{x}.$$

consistent with the Γ-limit found in Gioia & James [16]. For a more thorough analysis of this thin film model we refer to De Simone *et al.* [10, 11].

11 Appendix C: One-dimensional reduction

From this two dimensional magnetostatic energy functional, we can recover the one-dimensional magnetostatic energy functional introduced by Aharoni [1] for the study of one-dimensional walls.

In the one-dimensional case, we would consider magnetization distributions independent of the variable y. Consider a domain which is infinite in the x and y directions, but has finite thickness. We obtain the model for the one-dimensional case by assuming that the y direction is finite of length L, and then letting $L\to\infty$. In that case, the natural quantity to look at would be the averaged energy: $E = \frac{1}{2L}E_M$. If $\mathbf{m} = \mathbf{m}(x)$, the two dimensional

Downloaded from https://www.cambridge.org/core. Lehrst F Alte Geschichte Hist Inst, on 06 Jun 2017 at 07:46:52, subject to the Cambridge Core terms of use, available at https://www.cambridge.org/core/terms. https://doi.org/10.1017/S0956792504005595

Fourier transform becomes:

$$\mathscr{F}(\mathbf{m})(\xi_1,\xi_2) = \widehat{\mathbf{m}}(\xi_1)\frac{\sin(2\pi\xi_2 L)}{\pi\xi_2}, \tag{11.1}$$

where $\widehat{\mathbf{m}}$ and $\mathscr{F}(M)$ represent the corresponding Fourier Transform in one and two dimensions respectively.

We substitute in the two dimensional energy functional, and average in the y direction:

$$\begin{aligned} 2E_M[\mathbf{m}] = \frac{1}{2L}\int_{\mathbb{R}^2} \frac{\xi_1^2\widehat{\mathbf{m}}_1^2(\xi_1) + 2\xi_1\xi_2\widehat{\mathbf{m}}_1(\xi_1)\widehat{\mathbf{m}}_2(\xi_1) + \xi_2^2\widehat{\mathbf{m}}_2^2(\xi_1)}{\xi_1^2+\xi_2^2}\frac{\sin^2(2\pi\xi_2 L)}{\pi^2\xi_2^2}(1-\widehat{\Gamma}_\delta(|\xi|))\,d\xi_1\,d\xi_2 \\ + \frac{1}{2L}\int_{\mathbb{R}^2}\widehat{\mathbf{m}}_3^2(\xi_1)\frac{\sin^2(2\pi\xi_2 L)}{\pi^2\xi_2^2}\widehat{\Gamma}_\delta(|\xi|)\,d\xi_1\,d\xi_2 \end{aligned} \tag{11.2}$$

We can write

$$\phi_L(\xi) = \frac{\sin^2(2\pi\xi_2 L)}{2L\pi^2\xi_2^2} = 2L\phi_1(2L\xi_2),$$

where

$$\phi_1(\xi) = \frac{\sin^2(\pi\xi)}{\pi^2\xi^2}.$$

Using residues, one gets $\int_{\mathbb{R}}\phi_1(x)\,dx = 1$. Therefore, ϕ_L is an approximation to the identity in $\mathbb{R}$, so it is easy to take the limit $L\to\infty$:

$$\lim_{L\to\infty} E_M[\mathbf{m}] = \frac{1}{2}\int_{\mathbb{R}}\widehat{\mathbf{m}}_1^2(\xi_1)(1-\widehat{\Gamma}_\delta(|\xi_1|))\,d\xi_1 + \frac{1}{2}\int_{\mathbb{R}}\widehat{\mathbf{m}}_3^2\widehat{\Gamma}_\delta(|\xi_1|)\,d\xi_1,$$

which is precisely the one-dimensional self-induced energy.

References

[1] Aharoni, A. (1966) Energy of one dimensional domain walls in ferromagnetic films. *J. Appl. Phys.* **37**(8), 3271–3279.

[2] Bleistein, N. & Handelsman, R. A. (1975) *Asymptotic Expansions of Integrals.* Dover.

[3] Brown Jr., W. F. (1963) *Micromagnetics.* Interscience Tracts on Physics and Astronomy. Interscience.

[4] Choksi, R. & Kohn, R. V. (1998) Bounds on the micromagnetic energy of a uniaxial ferromagnet. *Comm. Pure Appl. Math.* **51**(3), 259–289.

[5] Choksi, R., Kohn, R. V. & Otto, F. (1999) Domain branching in uniaxial ferromagnets: a scaling law for the minimum energy. *Comm. Math. Phys.* (1999) **201**, 61–79.

[6] Collette, R. (1964) Shape and energy of néel walls in very thin ferromagnetic films. *J. Appl. Phys.* **35**(11), 3294–3301.

[7] Dal Maso, G. (1983) *Introduction to Γ-Convergence.* Progress in Nonlinear Differential Equations and their Applications. Birkhauser.

[8] Dennis Jr., J. E. & Schnabel, R. B. (1983) *Numerical Methods for Unconstrained Optimization and Nonlinear Equations.* Series in Computational Mathematics. Prentice-Hall.

[9] De Simone, A. (1993) Energy minimizers for large ferromagnetic bodies. *Arch. Rational Mech. Anal.* **125**, 99–143.

[10] De Simone, A., Kohn, R. V., Müller, S. & Otto, F. (1999) Magnetic microstructures – a paradigm of multiscale problems. *Proceedings ICIAM.*

Downloaded from https://www.cambridge.org/core. Lehrst F Alte Geschichte Hist Inst, on 06 Jun 2017 at 07:46:52, subject to the Cambridge Core terms of use, available at https://www.cambridge.org/core/terms. https://doi.org/10.1017/S0956792504005595

[11] De Simone, A., Kohn, R. V., Müller, S. & Otto, F. (2004) Repulsive interaction of Néel walls, and the internal length scale of the cross-tie wall. *Multiscale Modeling and Simulation.*
[12] Dietze, H. D. & Thomas, H. (1961) *Z. Physik*, **163**, 523.
[13] García-Cervera, C. J. (1999) *Magnetic Domains and Magnetic Domain Walls.* PhD thesis, Courant Institute of Mathematical Sciences, New York University.
[14] García-Cervera, C. J. & Weinan, E. (2000) Effective dynamics in thin ferromagnetic films. *J. Appl. Phys.* **90**(1), 370–374.
[15] García-Cervera, C. J., Gimbutas, Z. & Weinan, E. (2003) Accurate numerical methods for micromagnetics simulations with general geometries. *J. Comp. Phys.* **184**(1), 37–52.
[16] Gioia, G. & James, R. D. (1997) Micromagnetics of very thin films. *Proc. R. Soc. Lon. A*, **453**, 213–223.
[17] Holz, A., Hartung, W. & Hubert, A. (1969) *Z. angew Phys.* **26**, 145.
[18] Hubert, A. (1969) Stray-field-free magnetization configurations. *Phys. Stat. Sol.* **32**, 519–534.
[19] Hubert, A. & Schäfer, R. (1998) *Magnetic Domains: The Analysis of Magnetic Microstructures.* Springer-Verlag.
[20] Landau, L. & Lifshitz, E. (1935) On the theory of the dispersion of magnetic permeability in ferromagnetic bodies. *Physikalische Zeitschrift der Sowjetunion*, **8**, 153–169.
[21] Riedel, R. & Seeger, A. (1971) Micromagnetic treatment of Néel walls. *Phys. Stat. Sol. (B)*, **46**, 377–384.
[22] Thakkar, A. J. & Smith Jr., V. H. (1975) A strategy for the numerical evaluation of Fourier sine and cosine transforms to controlled accuracy. *Comput. Phys. Comm.* (10), 73–79.
[23] Wang, X.-P., García-Cervera, C. J. & Weinan, E. (2001) A Gauss-Seidel Projection Method for the Landau-Lifshitz equation. *J. Comp. Phys.* **171**, 357–372.

Downloaded from https://www.cambridge.org/core. Lehrst F Alte Geschichte Hist Inst, on 06 Jun 2017 at 07:46:52, subject to the Cambridge Core terms of use, available at https://www.cambridge.org/core/terms. https://doi.org/10.1017/S0956792504005595